NASA TECHNICAL NOTE

NASA TN D-3566

NASA TN D-3566

EXPERIMENTAL ROCKET PERFORMANCE OF APOLLO STORABLE PROPELLANTS IN ENGINES WITH LARGE AREA RATIO NOZZLES

by Carl A. Aukerman and Arthur M. Trout

Lewis Research Center
Cleveland, Ohio

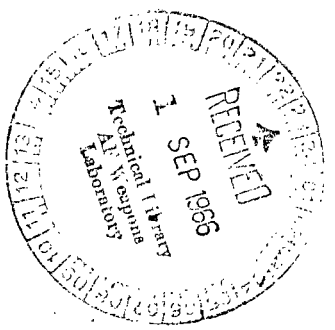

NATIONAL AERONAUTICS AND SPACE ADMINISTRATION • WASHINGTON, D. C. • AUGUST 1966

EXPERIMENTAL ROCKET PERFORMANCE OF APOLLO STORABLE PROPELLANTS IN ENGINES WITH LARGE AREA RATIO NOZZLES

By Carl A. Aukerman and Arthur M. Trout

Lewis Research Center
Cleveland, Ohio

NATIONAL AERONAUTICS AND SPACE ADMINISTRATION

For sale by the Clearinghouse for Federal Scientific and Technical Information
Springfield, Virginia 22151 – Price $2.00

EXPERIMENTAL ROCKET PERFORMANCE OF APOLLO STORABLE PROPELLANTS IN ENGINES WITH LARGE AREA RATIO NOZZLES

by Carl A. Aukerman and Arthur M. Trout

Lewis Research Center

SUMMARY

The performance of nitrogen tetroxide and a blend of 50 percent hydrazine and 50 percent unsymmetrical dimethyl hydrazine (UDMH) was evaluated at a chamber pressure of 100 pounds per square inch absolute in rocket engines with large area ratio nozzles which produced 8000 to 9000 pounds of thrust. Two contoured nozzles with area ratios of 60 and 40 plus a 15° conical nozzle with an area ratio of 60 were operated at mixture ratios between 1.4 and 2.2. Tests were also run with 1.3-area-ratio nozzles to determine the most reliable and accurate method of separating internal performance between the combustion chamber and supersonic nozzle. Attempts were made to improve nozzle performance experimentally by injecting a catalytic fluid and analytically by recontouring the supersonic portion.

The maximum delivered vacuum impulse at a mixture ratio of 2.0 was 320 seconds for the conical nozzle and 318 for the scaled Apollo Service Module nozzle with an area ratio of 60. The injector used was designed at Lewis Research Center and produced a characteristic velocity c* efficiency of 98 percent for these tests. The transtage contoured nozzle with an area ratio of 40 delivered 308 seconds of vacuum impulse using an injector of 97 percent c*. Experimental thrust coefficients indicated that some degree of equilibrium flow existed and the net value could be predicted by aerodynamic and chemical reaction kinetic analysis. Nozzle performance was shown to be unaffected by c* variations and by combustion instability. The two attempts to improve performance were not successful.

Measurements of pressures in the combustion chamber proved to be very unreliable for use in calculating chamber or nozzle performance. The use of impulse measurements with a low area ratio nozzle to calculate c* efficiency was the most reliable and accurate method.

INTRODUCTION

The use of nitrogen tetroxide (N_2O_4) and a blend of 50 percent hydrazine and unsymmetrical dimethyl hydrazine (50-50 fuel blend) as a rocket propellant for upper stages has increased markedly in the last several years. It was a logical step in advancing from the first generation propellants to the ultimate high energy combinations in that a compromise between performance and problem areas was achievable. As with any new advance, however, all aspects involving the use of these propellants had to be investigated to determine actual performance capability and to provide adequate knowledge for system design. The decision to use these storable propellants in the NASA Apollo program for manned lunar exploration placed tremendous emphasis on solving three major problems associated with the propulsion systems. These areas, which required additional study, were (1) combustion instability, (2) ablative thrust chamber durability, and (3) overall engine performance. The first two of these problems were encountered early, and much effort was directed toward their study and solution. However, the verification of complete engine performance and particularly nozzle performance was not obtained in the early stages because of the difficulty of acquiring suitable hardware and access to an altitude test facility. The probable influence of nonequilibrium chemistry on nozzle performance could not be defined theoretically and was uncertain for the Apollo mission requirements. It was this lack of information on nozzle efficiency with these propellants that brought about the program at Lewis Research Center reported herein.

Experimental programs have been conducted in the past to study nozzle performance with propellants that were affected by reaction kinetics (refs. 1 and 2) but no program involving N_2O_4 and this 50-50 fuel blend had been implemented. The only testing conducted at low chamber pressure and high area ratio with these propellants was with a 2200-pound-thrust engine (refs. 3 and 4) and resulted in impulse measurements considerably below the expected values. The USAF-SSD had sponsored the Titan transtage engine with 8000 pounds of thrust, a chamber pressure of 100 pounds per square inch absolute, and an area ratio of 40 but altitude testing was yet to come. Numerous attitude control engines at the 100-pound thrust level were also under development but engine size was too small to shed light on the problem of nonequilibrium kinetics in the nozzle. A performance evaluation program was funded by NASA Manned Spacecraft Center (ref. 5), but this work was also done at a rather small scale of 1000 pounds thrust and was not undertaken until after the initiation of the program described herein. In order for the results to be directly applicable, the problem of nozzle performance had to be investigated within the range of engine sizes used in the Apollo system. The primary propulsion systems of the Apollo program are summarized in table I. (Symbols are defined in appendix A.)

The program undertaken at Lewis was intended to support the needs of the Apollo

TABLE I. - PRIMARY PROPULSION SYSTEMS

OF APOLLO PROGRAM

Propulsion system	Thrust, F, lb	Oxidant-to-fuel ratio, O/F	Combustion chamber pressure, P_c, psia	Area ratio, ϵ_e
LEM[a] ascent	3 500	1.6	120	45.6
LEM[a] descent	10 500 to 1050	1.6	110	49.0
Service Module	21 000	2.0	100	62.5

[a]Lunar Excursion Module.

propulsion systems by fulfilling the following objectives at the 9000-pound thrust level:

(a) Determine the impulse capability of N_2O_4 and the 50-50 fuel blend

(b) Identify internal engine performance (c* and $C_{F,v}$)

(c) Study potential methods to improve performance

(d) Correlate results with best available analytical tools

The experimental approach was to evaluate several injectors in a standard chamber with a low area ratio nozzle in order to obtain maximum performance with stable combustion and then determine overall performance in engines with large area ratio nozzles. The testing to evaluate injector performance also provided sufficient information to evaluate different nozzle throat total pressure calculation procedures, thereby permitting identification of the contribution to performance of the injector, chamber (or subsonic expansion), and supersonic nozzle. Several methods of calculating throat total pressure were compared to ensure that the necessary accuracy and reliability were achieved.

The injector evaluations are presented as calibration curves of characteristic velocity efficiency as a function of mixture ratio. The specific impulse data from the engine performance runs with the large area ratio nozzles can then be used with the c* calibration curves to accurately determine the thrust coefficients for these nozzles. This division of overall performance simplified the study of potential improvement and correlation of results.

The tests were run at a nominal throat total chamber pressure of 100 pounds per square inch absolute over an oxidant-to-fuel mixture ratio range from 1.4 to 2.2. Three triplet injectors were evaluated in heat sink chambers with L^* from 12.7 to 62.5 inches. The contraction ratio was 1.9, and the nozzle expansion area ratio was 1.3. All chambers except two were of conventional cylindrical shape; these two were conically tapered from the injector face to the throat. The basic nozzle throat diameter was 7.82 inches (48 sq in. in area), which resulted in thrust of 6000 to 9000 pounds, depending on the

supersonic section of the nozzle. The large area ratio nozzles used for this program were the following:

(1) Area-ratio-60, 15^{o} conical

(2) Area-ratio-60, Service Module Propulsion System (SPS) contour (scaled)

(3) Area-ratio-40, Titan transtage contour

Data were also obtained with the SPS contour terminated at $\epsilon = 5.0$, which was an assembly joint. Attempts were made to improve nozzle performance by injecting a third fluid into the mainstream near the throat to act as a catalyst and maintain equilibrium flow to a large area ratio. Analytical studies were also conducted to determine if recontouring of the nozzle would extend the region of equilibrium flow. Documentation was also made of the effect of combustion instability on the nozzle thrust coefficient C_F.

APPARATUS

Facility

The program was conducted in an altitude test facility that was capable of maintaining ambient pressures down to 30 to 40 pounds per square foot absolute during engine firings. A schematic of this installation and general arrangement of the entire test cell is shown in figure 1. Several problems associated with the testing of low area ratio nozzles in an

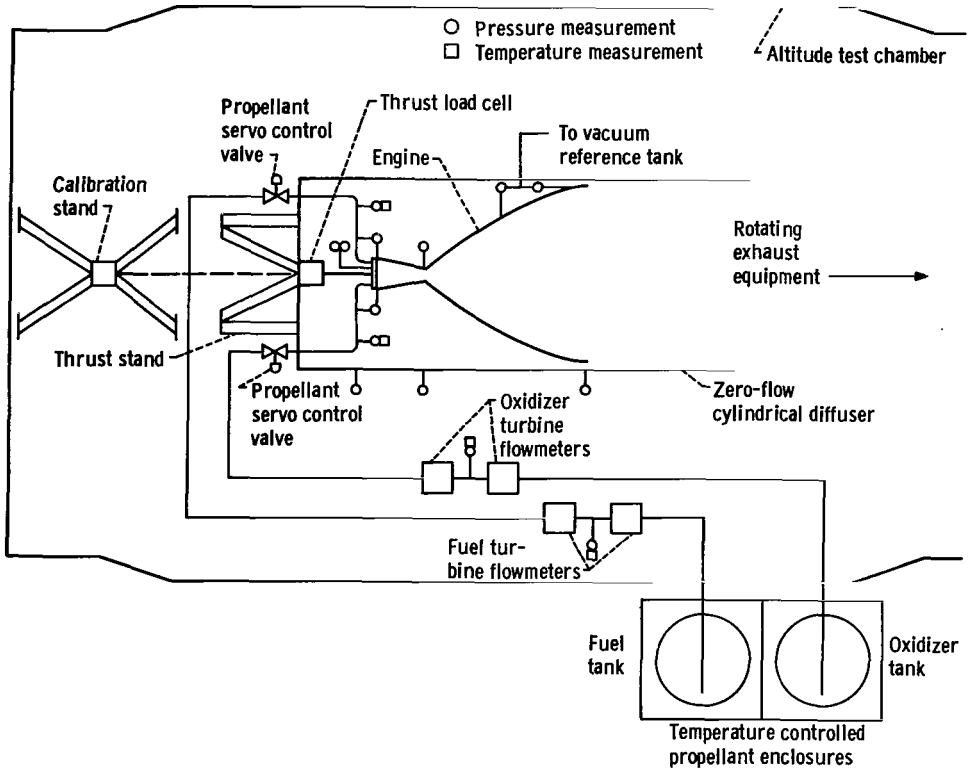

Figure 1. - Schematic of test setup.

altitude facility were overcome by firing into the 14-foot-diameter test section without a flame collector tube. This arrangement was necessary for two reasons: If a flame tube completely enclosed the engine, the high exhaust pressure of the nozzle caused excessive recirculation of hot gases. Secondly, if an open flame tube were used, ejector action of the exhaust gases induced secondary airflow over the engine which altered the thrust readings. With the resolved configuration, the highest possible test section pressure was desired but this was limited to 750 pounds per square foot absolute by personnel and equipment safety restrictions. With large area ratio nozzles, tests were run at maximum altitude with the engine firing into a 72-inch-diameter cylindrical diffuser, which encapsuled the entire engine and thrust system. The photograph of figure 2 shows the test cell and large area ratio engine installation with the diffuser rolled downstream.

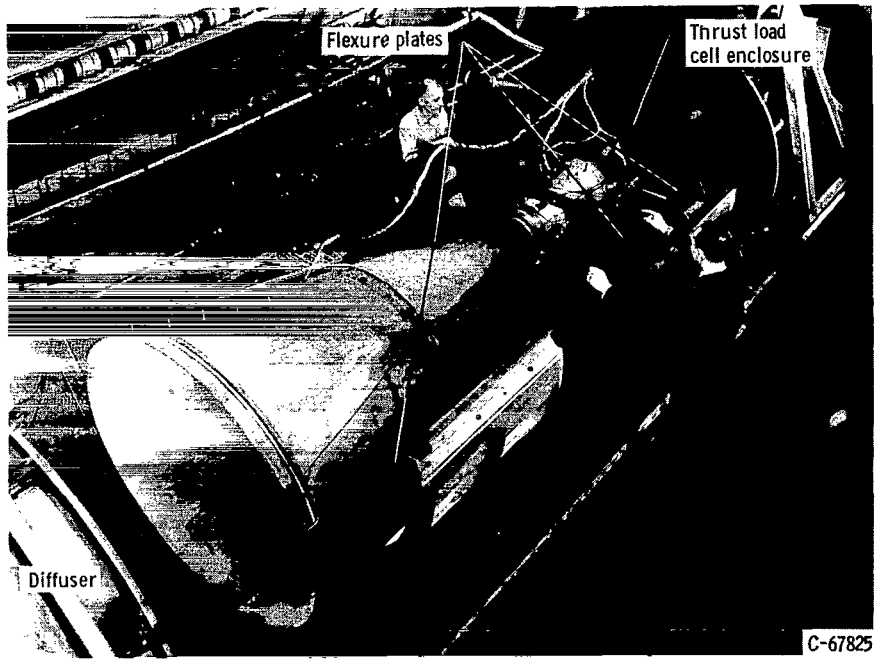

Figure 2. - Normal installation of large area ratio engine.

Propellant Supply System

The fuel and oxidizer propellant supply systems, also included in figure 1, were functionally identical. Run tanks were located outside of the building in temperature controlled enclosures to maintain the propellants within the limits of storability to prevent freezing and separation of the fuel and dissociation of the oxidizer. Propellants were expelled from the tanks through dip tubes by pressurizing with nitrogen. Two turbine flowmeters in series were used for flow measurement of each system.

The flow control loop for each system included an electronic controller, a servo control valve, and one of the flowmeters. Output from the flowmeter was continuously compared to the desired preset flow by the controller which supplied an error signal to position the servo valve. Sensing mixture ratio, chamber pressure, or thrust was avoided to simplify the system and thereby make it more reliable and stable.

Engines

Combustion chambers. - All combustion chamber hardware was of a heat sink design fabricated from mild steel and flame sprayed on the inside with a 0.012-inch nichrome base under a 0.018-inch aluminum oxide thermal barrier. This permitted 10 to 20 runs of 6 seconds maximum duration before refurbishment of the surface was required because of the onset of breakdown of the Al_2O_3 surface. Heat transfer losses and thermal expansion are negligible for short runs with this configuration.

Both cylindrical and conical shaped combustion chambers were used. The cylindri-

TABLE II. - GEOMETRY OF COMBUSTION CHAMBERS

[D_e = 8.92 in.; R_t = 3.91 in.; α = 15°.]

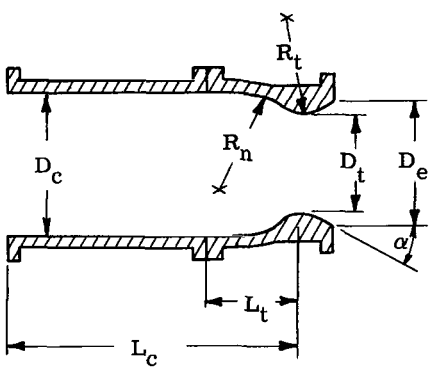

Cylindrical chamber

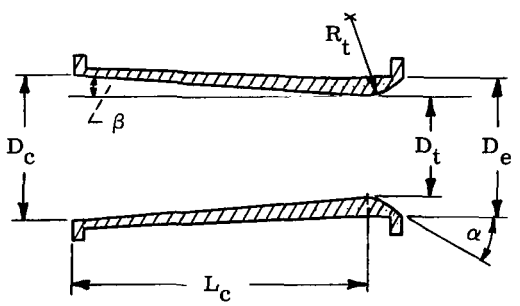

Conical chamber

Engine section		D_c, in.	D_t, in.	L_c, in.	R_n, in.	L_t, in.	β, deg	ϵ_c	ϵ_e	L^*, in.
Throat	-0	10.77	7.82	------	7.82	7.94	---	1.897	1.301	12.7
Cylindrical	-1	10.77	7.82	[a]18.44	7.82	----	---	1.897	1.301	[a]32.6
	-2	↓	↓	[a]23.69	↓	----	---	↓	↓	[a]42.6
	-3	↓	↓	[a]28.94	↓	----	---	↓	↓	[a]52.5
	-4	↓	↓	[a]34.19	↓	----	---	↓	↓	[a]62.5
	-5	11.91	↓	[a]23.69	↓	----	---	2.320	↓	[a]45.9
Conical	-6	10.77	7.82	22.01	----	----	3.9	1.897	1.301	31.3
	-7	11.91	7.48	17.72	----	----	7.2	2.535	1.422	30.1

[a]Dimension includes throat section.

cal chamber assembly consisted of a convergent-divergent throat section to which cylindrical spoolpieces could be bolted to extend the combustion chamber length. Conical chamber and throat sections were fabricated in one piece. The chamber hardware is described in detail in table II; basically, all chambers but two had a contraction ratio of 1.9, a throat area of 48.0 square inches, and a 15^{o} conical nozzle with an expansion area ratio of 1.3. The exceptions were the -5 and -7 chambers used with injector B. Chamber lengths ranged from 7.94 (throat section) up to 34.19 inches corresponding to an L^{*} range of 12.7 to 62.5 inches.

Nozzles. - The large area ratio nozzles were also heat sink, mild steel designs. The 15^{o} conical nozzle skirt could be attached to any of the chambers just described, whereas the two contour nozzles were final machined with a specific chamber. Figure 3 is a photograph of the three engine assemblies without injectors. A complete list of the X and Y coordinates for these two contoured engines appears in table III. The Al_2O_3 nichrome thermal protection was faired out at an area ratio of 10.0 for the conical nozzle and as noted in table III.

Both contour nozzle designs were taken from active engine development programs. The area-ratio-60 nozzle was scaled from the NASA Apollo SPS and also truncated from the design area ratio of 62.5. The area-ratio-40 nozzle was identical, supersonically, to the USAF-SSD Titan transtage engines. These contours were computed using the method of characteristics and the optimization technique of Rao for operation in a vacuum. Some

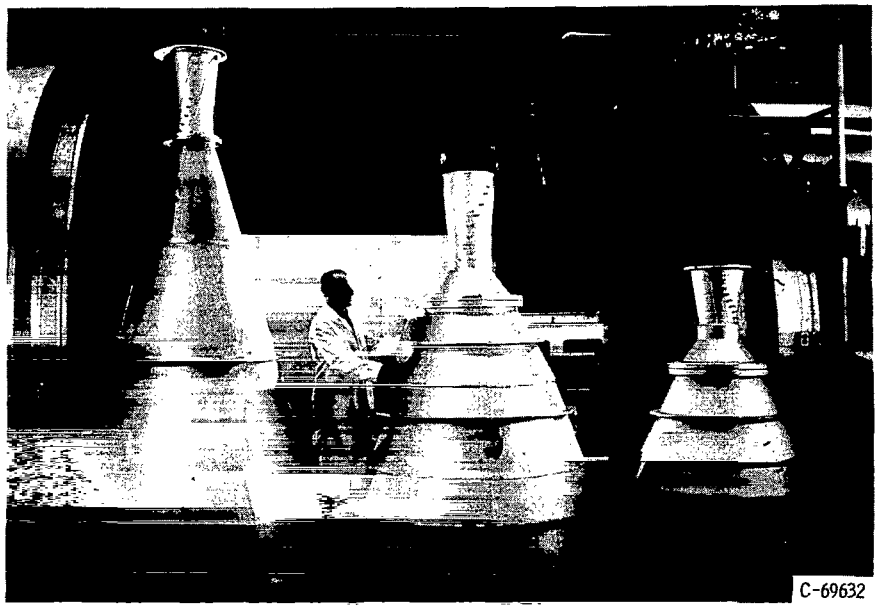

(a) Area-ratio-60; 15° conical. (b) Area-ratio-60; SPS contour. (c) Area-ratio-40; Titan transtage contour.

Figure 3. - Three primary heat sink nozzles with chambers attached.

TABLE III. - COORDINATES OF CONTOUR NOZZLES

(a) Service module propulsion system

X	Y	X	Y	X	Y	X	Y
0.000	3.910	11.500	10.970	25.500	18.040	41.000	23.700
.400	3.930	12.000	11.270	26.000	18.250	42.000	24.010
.800	3.999	12.500	11.565	26.500	18.450	43.000	24.310
1.000	4.038	13.000	11.875	27.000	18.655	44.000	24.615
1.200	4.098	13.500	12.146	27.500	18.860	45.000	24.910
1.400	4.168	14.000	12.431	28.000	19.065	46.000	25.200
1.600	4.252	14.500	12.701	28.500	19.265	47.000	25.480
1.800	4.351	15.000	12.976	29.000	19.465	48.000	25.765
2.000	4.465	15.500	13.251	29.500	19.660	49.000	26.040
2.200	4.594	16.000	13.516	30.000	19.855	50.000	26.310
2.500	4.813	16.500	[a]13.781	30.500	20.050	51.000	26.575
3.000	5.188	17.000	14.040	31.000	20.245	52.000	26.835
3.500	5.563	17.500	14.300	31.500	20.435	53.000	27.090
4.000	5.933	18.000	14.555	32.000	20.620	54.000	27.345
4.500	6.303	18.500	14.810	32.500	20.810	55.000	27.595
5.000	6.663	19.000	15.060	33.000	20.990	56.000	27.835
5.500	7.023	19.500	15.305	33.500	21.175	57.000	28.075
6.000	7.383	20.000	15.550	34.000	21.370	58.000	28.310
6.500	7.728	20.500	15.790	34.500	21.530	59.000	28.540
7.000	8.074	21.000	16.030	35.000	21.705	60.000	28.770
7.500	8.419	21.500	16.265	35.500	21.875	61.000	29.000
8.000	8.749	22.000	16.500	36.000	22.050	62.000	29.220
8.500	9.079	22.500	16.735	36.500	22.225	63.000	29.435
9.000	9.404	23.000	16.960	37.000	22.395	64.000	29.650
9.500	9.730	23.500	17.190	37.500	22.565	65.000	29.855
10.000	10.040	24.000	17.410	38.000	22.730	66.000	30.065
10.500	10.360	24.500	17.625	39.000	23.060	67.000	30.270
11.000	10.660	25.000	17.835	40.000	23.380	67.140	30.287

[a]End of thermal protection.

TABLE III. - Concluded. COORDINATES OF CONTOUR NOZZLES

(b) Titan transtage

X	Y	X	Y	X	Y	X	Y
0.000	3.740	10.000	9.590	23.500	16.020	37.000	20.535
.200	3.750	10.500	9.885	24.000	16.215	37.500	20.675
.400	3.760	11.000	10.166	24.500	16.405	38.000	20.820
.600	3.790	11.500	10.446	25.000	16.600	38.500	20.955
.800	3.829	12.000	10.726	25.500	16.785	39.000	21.095
1.000	3.879	12.500	10.991	26.000	16.970	39.500	21.230
1.200	3.948	13.000	[a]11.256	26.500	17.150	40.000	21.360
1.400	4.023	13.500	11.510	27.000	17.335	40.500	21.495
1.600	4.122	14.000	11.770	27.500	17.515	41.000	21.625
1.800	4.221	14.500	12.025	28.000	17.690	41.500	21.750
2.000	4.344	15.000	12.275	28.500	17.865	42.000	21.880
2.200	4.483	15.500	12.520	29.000	18.035	42.500	22.005
2.500	4.703	16.000	12.760	29.500	18.205	43.000	22.130
3.000	5.053	16.500	13.000	30.000	18.375	43.500	22.260
3.500	5.408	17.000	13.235	30.500	18.540	44.000	22.385
4.000	5.758	17.500	13.470	31.000	18.705	44.500	22.505
4.500	6.104	18.000	13.695	31.500	18.865	45.000	22.630
5.000	6.444	18.500	13.920	32.000	19.030	45.500	22.745
5.500	6.779	19.000	14.140	32.500	19.190	46.000	22.860
6.000	7.109	19.500	14.360	33.000	19.345	46.500	22.970
6.500	7.439	20.000	14.580	33.500	19.500	47.000	23.085
7.000	7.764	20.500	14.790	34.000	19.650	47.500	23.200
7.500	8.080	21.000	15.005	34.500	19.800	48.000	23.310
8.000	8.390	21.500	15.210	35.000	19.950	48.500	23.420
8.500	8.700	22.000	15.420	35.500	20.100	49.000	23.530
9.000	9.005	22.500	15.620	36.000	20.245	49.609	23.665
9.500	9.300	23.000	15.820	36.500	20.390		

[a]End of thermal protection.

TABLE IV. - SUMMARY OF NOZZLE DETAILS

$[R_t/Y_t = 1.0.]$

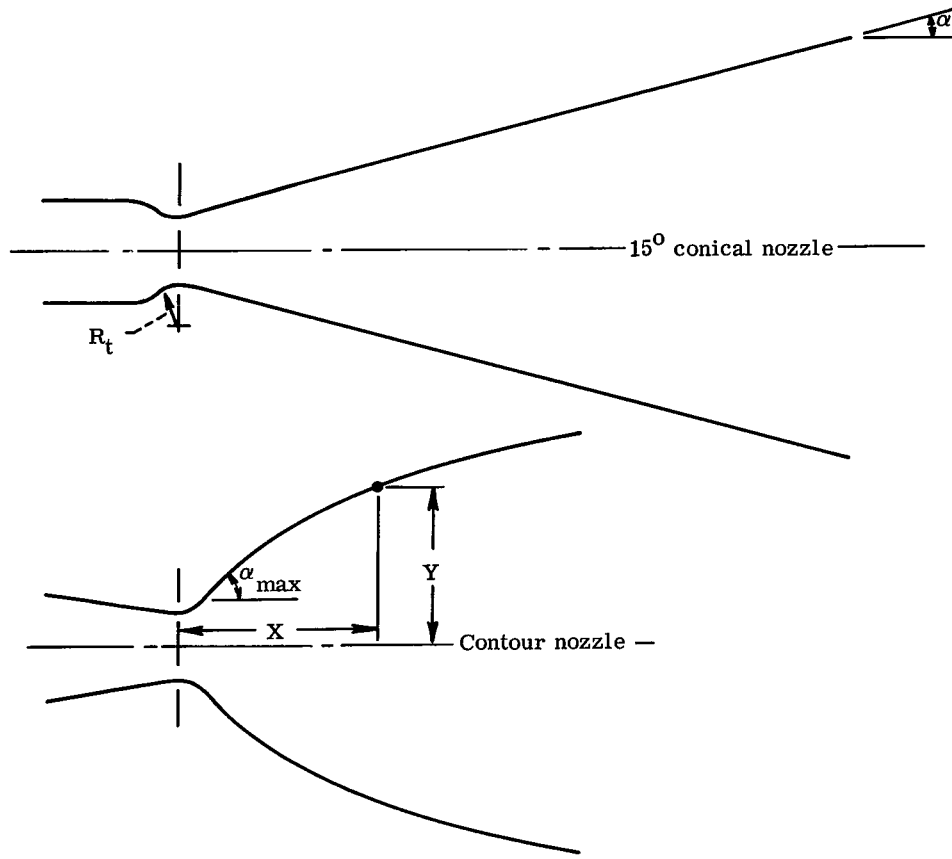

Nozzle	ϵ_e	α_e	α_{max}	X_e/Y_t	Percent bell
15° conical	60.9	15°	15°	25.42	100.5
SPS contour	60	11°9'	36°48'	17.17	67.9
Transtage contour	40	12°24'	35°44'	13.26	66.3

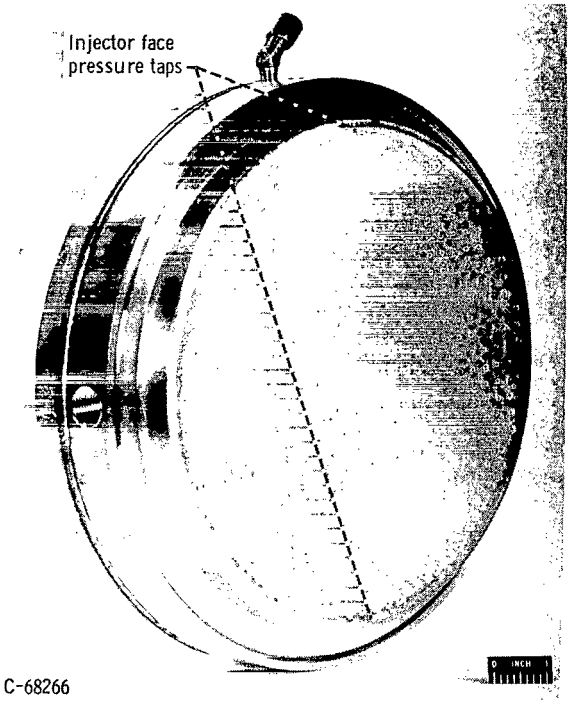

(a) Injector A: alternating grid triplet with 553 elements nominal.

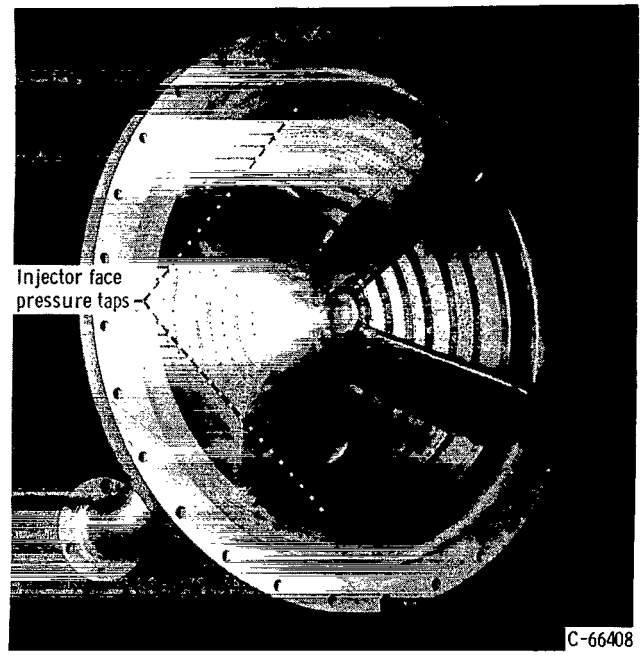

(b) Injector B: transtage triplet with 392 elements nominal.

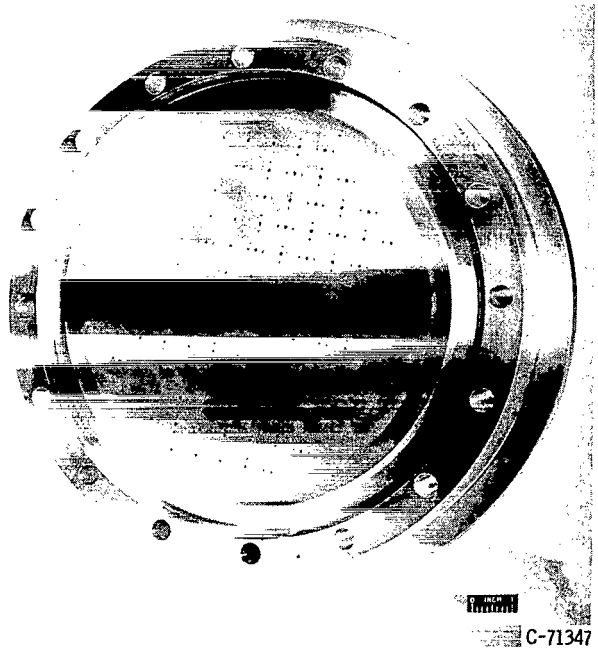

(c) Injector C: alternating grid triplet with 129 elements.

Figure 4. - Injectors chosen for program evaluation.

of the features of these nozzles are summarized in table IV. The two area-ratio-60 nozzles had throat areas of 48.0 square inches. For the Apollo SPS engine, this represents a scaledown to 39.5 percent of the throat area of the full-scale engine. The area-ratio-40 nozzle had a throat area of 43.9 square inches, which corresponds to a full-scale transtage nozzle.

Injectors. - The required injector for this program had to deliver high performance with stable combustion to be acceptable as a gas generator for the large area ratio nozzle tests. Several injector configurations were designed inhouse and evaluated along with an injector acquired through the USAF-SSD Transtage Program. The latter was one of the early development versions which was known to be stable. Out of 13 injectors surveyed, three were chosen for complete evaluation and are pictured in figure 4. The Lewis designed injectors A and C were flat faced, unbaffled, and employed inline triplet elements with a two fuel on one oxidizer jet arrangement. The transtage injector B was spherical faced, baffled, employed triangularly arranged elements in the triplet with basically two oxidizer jets on one fuel, and was 1.2 inches larger in diameter than injectors A and C. Table V describes the details of the orifice patterns.

TABLE V. - DETAILS OF INJECTOR ORIFICE PATTERNS

		Injector		
		A	B	C
Number of holes	Oxidizer	[a]553	784	129
	Fuel	[a]1160	[a]432	258
Diameter of holes, in.	Oxidizer	0.035	[b]0.029	0.0785
	Fuel	.0225	[b].031	.043
Total flow area, sq in.	Oxidizer	0.532	0.603	0.624
	Fuel	.461	.417	.375
Impingement angle, deg		30	(c)	40
Impingement distance, in.		0.58	(c)	0.56
Velocity ratio, [d] V_O/V_F		1.09	0.87	0.76
Method of cooling face		Fuel	Fuel and oxidizer[e]	Oxidizer

[a]Includes film cooling or showerhead elements around circumference.

[b]Nominal hole diameter.

[c]Complexity does not warrant detail description.

[d]Based on O/F = 2.0.

[e]Baffles also fuel cooled.

Special Hardware

Throat total pressure probe. - One of the approaches to determine the most reliable and accurate method of separating combustion chamber and nozzle performance was to measure the throat total pressure directly. The probe that evolved after numerous tests is shown in figure 5. The probe itself is thick-walled stainless steel tubing, while the support which also protects the tubing was mild steel. This design was adequate to endure approximately 2 seconds of exposure in the throat at full chamber pressure. Total durations exceeding 6 seconds could be obtained by slipping a Teflon or boron nitride sleeve over the probe if care were taken to provide extra protection at the base of the probe by using additional material.

Streak-photography setup. - Streak photography was attempted as a method of obtaining an axial velocity profile as the gases proceeded along the chamber. An axial slit 1/4 inch wide was cut into several chambers and sealed with a Lucite window. During a typical firing, a high-speed continuous exposure camera ran film perpendicular to the window at speeds up to 100 feet per second. The setup for streak photography is also shown in figure 5. After development and printing of the film, the angle of the gas streaks

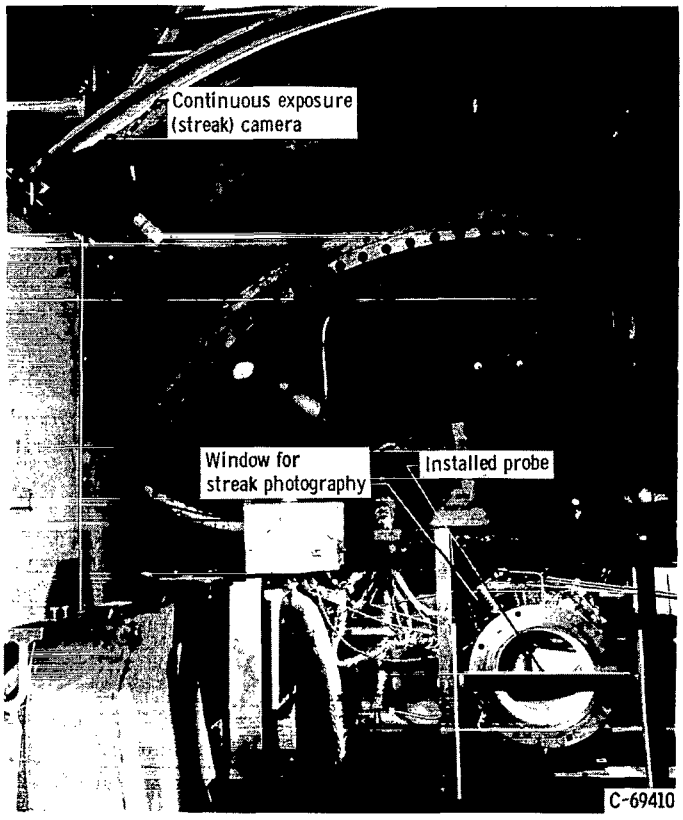

(a) Streak photography setup.

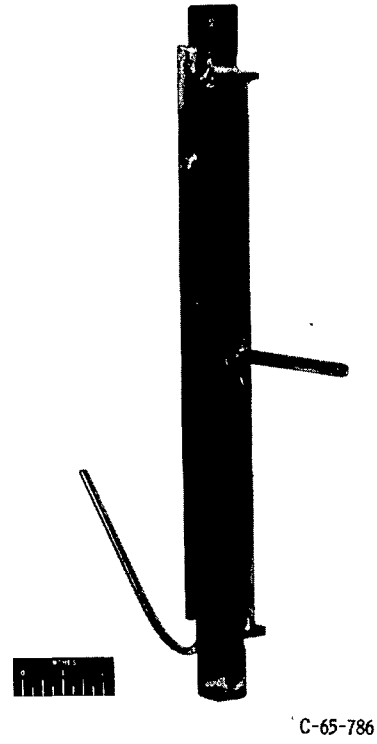

(b) Throat total pressure probe.

Figure 5. - Special hardware.

could be expressed as gas velocity by knowledge of the film speed and a scale factor.

Catalyst injection system. - A system was installed in the scaled Apollo SPS engine to inject a third fluid or catalyst into the gas stream for the purpose of improving performance by catalyzing the recombination process. This injection system consisted of four spray bars inserted through the walls of the chamber approximately 2 inches upstream of the throat. Several orifice arrangements were tried in order to obtain maximum penetration and distribution of the third fluid. Various spray bars contained one to five orifices, which were directed perpendicular to the flow in addition to a single orifice per spray bar directed upstream. The third fluid was supplied from a nitrogen pressurized tank when benzene was used and from a standard gas bottle when ethylene was used. The spray bars were self-cooled as long as the fluid was being injected.

Instrumentation

Locations of all major instrumentation are shown in figure 1 (p. 4).

Flow measurement. - Flow rates were measured with two turbine-type flowmeters (employing sleeve bearings) mounted in series in each propellant system. The alternating current signal from each meter was fed into a converter which provides a direct current output signal that is proportional to the input frequency. This signal was then available for digital processing and the servocontrol system. The original signal was also recorded directly on an oscillograph for control room monitoring. Pressure and temperature measurements at the flowmeters were used to calculate the fluid density. This was necessary since an 8° R temperature change will change oxidizer density by 1 percent and 20° R change will effect fuel density 1 percent.

Some doubt exists with regard to the adequacy of water calibrations for turbine flowmeters used in nitrogen tetroxide. For this reason, the two flowmeters scheduled for use in this program were sent to an independent calibrating source to be calibrated in N_2O_4. At the conclusion of testing, the oxidizer meters were recalibrated in both water and N_2O_4. Calibrations of the 2-inch meter in N_2O_4 before and after the program demonstrated extremely good repeatability and probably within 1/8 percent of the postrun water calibration up to the maximum normal range of operation. With the $1\frac{1}{2}$-inch meter, the postrun N_2O_4 calibration factor was 1/2 percent higher than the prerun value, with the water calibrations scattering in between. Comparison of the outputs obtained during the program from these two series installed meters showed that flows using the postrun calibration with the $1\frac{1}{2}$-inch meter were exactly equivalent to flow rates calculated using either calibration for the 2-inch meter. None of the data were adjusted to comply with this postrun calibration information. Since both meters were averaged to obtain flow

rates, the oxidizer flow would actually be biased by 1/8 percent and total flow in error by less than 1/10 percent. The conclusion from this effort was that the bias between a water calibration and a N_2O_4 calibration is barely perceptible (at least for meters greater than $1\frac{1}{2}$ in. in diam.) and its effect on total flow and performance is even less. A similar procedure was followed in calibrating the two fuel flowmeters in water and fuel. Data from the two fluids were within ±1/8 percent for both meters.

Thrust measurement. - The net thrust delivered by this installation was measured with a double bridge, strain gage load cell in compression. The weight of the engine assembly was supported by four or six flexure plates depending on the configuration. The complete engine and thrust system were encapsulated within the diffuser can to avoid any external drag. In this manner, essentially all of the net thrust was measured by the load cell. The small remainder was taken up in deflection of propellant lines, flexure plates, and instrumentation lines and was accounted for by the calibration. The calibration for total net thrust was obtained by loading the thrust system with a hydraulic cylinder and reading the true applied load with a proving ring deflection unit that was calibrated by the National Bureau of Standards. Repeatability of thrust calibrations was within ±1/4 percent. Gross vacuum thrust involved the addition of a pressure-area term (eq. (2)), which was about 2.0 percent of the gross value.

Pressure measurement. - Conventional steady-state pressure measurements were made with strain gage element transducers. The altitude environment required the transducers to have variable reference pressure capability, preferably of the differential pressure design to protect the element. Transducers measuring the higher pressures were referenced to the capsule or altitude chamber whereas the lower range pickups, including those for the capsule and altitude chamber, were referenced to a controlled vacuum system. Bench calibrations were made prior to installation of all transducers and periodic inplace calibrations were performed as an ultimate test. The latter was accomplished by attaching a plate to the low area ratio nozzle exit and pressurizing the engine with nitrogen gas. Readouts from the transducers involved were then processed through the digital data acquisition and reduction system. Readings that were in excess of ±1/2 percent were cause for rejection and replacement of the transducer.

The pressure oscillations associated with high-frequency combustion instability were measured with flush mounted high-frequency transducers that were mounted in water cooled adapters. Only the frequency and amplitude of the pressure oscillations were of interest, and the precision of a calibration was not warranted.

Temperature measurements. - Iron-constantan thermocouples referenced to a 150° F oven were used to measure propellant temperatures at the flowmeters and injector manifold.

Data acquisition. - Three readout systems were used to record the data from all of the instrumentation just described.

Two oscillographs containing about 36 channels of information were maintained in the control room. These were used to obtain preliminary data between firings in order to follow closely the progress of the testing. This system was essential for monitoring the tests and invaluable in signalling and locating problems such as faulty instrumentation or equipment.

The primary data were recorded with a digital system using a 4-kilocycle sweep rate over a block of 64 channels of information, thus providing data availability every 0.016 second. Data were recorded on magnetic tape and processed through a computer program. Terminal calculations were made every 0.256 second using data smoothed over 25 blocks for steady-state calculations. Basic parameters such as thrust, flow rate, and chamber pressure were sensed more than once per block. Calibration of this system was accomplished by maintaining all electronics in a linear input-output condition. Test cell instrument calibrations then apply directly.

Initial attempts for monitoring the high frequencies of combustion instability were made with a simple microphone in the test cell feeding an AM tape recorder. This approach was completely inadequate and led to the use of the sophisticated high-frequency response transducer system. The most convenient readout method for the needs of this program was an oscilloscope with an integrally mounted camera. The signal was split and triggered for display at two different sweep rates. At 0.5-second-per-centimeter sweep rate, the entire run was recorded and duration of screech observed. At 0.1 millisecond per centimeter, one instant of the run was expanded to show the wave form, amplitude, and frequency. A time exposure recorded both traces.

METHODS AND PROCEDURE

The methods of calculating internal performance of a rocket engine are worth discussing in order to point out certain deficiencies and problem areas that reflect on the accuracy of the final results.

By definition, the three primary rocket performance parameters are related by

$$I_v g = c^* C_{F,v} \tag{1}$$

where I_v and $C_{F,v}$ are calculated using vacuum thrust, defined as

$$F_v = F_m + P_a A_e \tag{2}$$

Experimentally these parameters are usually determined from measurements of thrust, total flow rate, and chamber pressure, with the latter corrected to the equivalent

of throat stagnation pressure. The relation of these basic parameters according to equation (1) becomes

$$\left(\frac{F_v}{\dot{w}}\right)g = \left(\frac{P_t A_t g}{\dot{w}}\right)\left(\frac{F_v}{P_t A_t}\right) \tag{3}$$

Since the terms in equation (3) are defined at the geometric throat, a clear separation between combustion chamber and nozzle performance exists at the nozzle throat; therefore, c* becomes a measurement of the performance of all processes in the chamber and not just combustion performance. Any subsonic flow losses or thermal losses must also be considered as c* deficiencies.

By inspection of equation (3) it is seen that errors in the product $P_t A_t$ affect c* directly and $C_{F,v}$ inversely but have no effect on impulse. This reversal of influence tends to give misleading results when problems of determining the product $P_t A_t$ arise, particularly when any errors are biased and not random. Corrections can be applied to the geometric or measured throat area to account for thermal expansion and for a flow coefficient but such corrections will vary from one type of chamber to another and are, therefore, legitimate c* deficiencies for that system. Examples of differences affecting these corrections are ablative as opposed to regenerative cooling, cylindrical as opposed to conical chambers, and conventional as opposed to tubular throats. In the program described herein, the thermal effects were minimized by the Al_2O_3 coating and the short run durations. The losses attributed to flow coefficient were minimized by the DeLaval nozzle design and should have been the classical three-dimensional value of 0.994 as often measured with air (ref. 6) and hot combustion products (ref. 7). However, in keeping with the definitions implied by equations (1) and (3), no such corrections were made to c*.

As a result, the entire problem of separation of c* performance from $C_{F,v}$ performance lies in the ability to consistently and reliably determine the throat total pressure. Several methods for calculating throat total pressure were considered so that a comparison of the results would indicate the best method to adopt. The different methods attempted were as follows:

(1) Measure head end pressure (through injector face) and correct to throat total pressure. The equation used was derived from the momentum equation written between the injector face and the nozzle entrance for the constant area chamber. Manipulating the terms to utilize rocket performance parameters results in

$$P_{t,c} = P_{i,c}\left(\frac{p_n}{P_n} + \frac{I_n g - V}{c^*_T \epsilon_c}\right)^{-1} \tag{4}$$

The terms p_n/P_n, I_n, and c^*_T were obtained from the theoretical calculations described in appendix B.

(2) Calculate throat total pressure from theoretical thrust coefficient and vacuum thrust from tests with a low area ratio nozzle; that is,

$$P_{t,F} = \frac{F_v}{C_{F,v} A_t} \tag{5}$$

(3) Measure throat total pressure directly with a probe located near the sonic point.

(4) Calculate a total pressure profile from the injector face to the throat using static pressure measurements and velocity head derived from streak photography.

In general, the approaches that required static pressure measurements were not necessarily considered trustworthy because of the numerous differences between the static environment of a bench calibration and the dynamic situation in a low contraction ratio chamber. The suspicions were that the transducer output was not necessarily indicative of the desired pressure even though the instrument was in apparent good order. Examples of factors that can confuse this reading are the following:

(a) Condition of the orifice

(b) Orientation of gas velocity to the orifice

(c) Nonuniform velocity distribution

(d) Gas recirculation zones

(e) High-frequency pressure fluctuations

(f) Leaks that develop during test

(g) Fluctuating ambient temperature surrounding transducer

(h) Unexpected behavior of the electronic systems

Undoubtably these problems are not everpresent, but the possibility of their existance cannot be ignored. By way of comparison, thrust load cells and turbine flowmeters (measuring incompressible fluids) are not subject to these dynamic effects and biases and thereby provide more direct readings for steady-state performance measurements.

The method described previously using equation (5) relies, of course, on the accurate calculation of the thrust coefficient. For the purpose of this program, the nozzle area ratio of 1.30 was chosen to ensure equilibrium expansion and to minimize frictional losses. The chemical kinetic calculations were done by a computer program, described in reference 8, that was based on the Bray criteria and indicated the freezing area ratio to be about 1.35 for the 15° conical nozzle. The actual vacuum thrust coefficient was calculated from an axisymmetric method of characteristics evaluation program and included frictional effects. The resulting vacuum thrust coefficient was 0.980 of the one-dimensional vacuum thrust coefficient for the 1.30-area-ratio nozzle.

RESULTS AND DISCUSSION

Determination of Throat Total Pressure

The results of the different methods to calculate throat total pressure had to be analyzed first since the ability to separate combustion chamber and supersonic nozzle performance was a prerequisite to the calculation procedure for the entire program. The documentation in figure 6 of the static pressures recorded in the chamber throughout the program quickly pointed out that these pressure measurements were unacceptable for performance calculations. Each part of figure 6 is a profile of static pressures as a function of distance from the injector face for $O/F = 2.0$. All pressure measurements were normalized to an arbitrary common flow rate of 29.0 pounds per second for comparison according to an equation $p' = p(29.0/\dot{w})$. For comparison of scatter only, the total pressure as calculated from a chamber tap measurement (eq. (4)) and from thrust (eq. (5)) is plotted at the throat station for each configuration with the number of data points that make up this band also noted. For reference, the isentropic pressure profile, calculated from one-dimensional isentropic expansion pressure ratio and $P_{t,F}$, was included in figure 6 for each configuration. The pressure profiles in the conical and cylindrical chambers of nominal $L^* = 32$ inches using the stable injector C are presented in figures 6(a) and (b). These two particular chambers were chosen because they produced the same c* efficiency, a fact that will be presented later. With the conical chamber, normalized pressures at the first wall static tap ranged from 99.0 to 104.8 pounds per square inch absolute or almost ±3 percent for 14 runs. This scatter was recorded with two transducers in parallel on the same tap. Although an injector face tap was not available with injector C to calculate throat total pressure by equation (4), indications are that no location would have recorded an acceptable repeatability for performance calculations. Equation (4) did not apply to data from the first tap but it was used to calculate $P_{t,c}$ for comparison to $P_{t,F}$ in lieu of a more rigorous approach. Therefore, a comparison can be made of the scatter using equations (4) and (5) but not the absolute level.

With the results shown in figure 6(b) using the cylindrical chamber, the scatter of data was not excessive. However, it was felt that a larger number of runs would have reproduced a wider band of uncertainty. A later discussion will show that a larger number of runs did not increase the scatter of thrust and impulse measurements.

The pressure profiles obtained with a cylindrical and a conical chamber using injector A are shown in figures 6(c) and (d). Although high-frequency instrumentation used later in the program proved this injector to be unstable in the second tangential mode (3960 cps), the pressure data were included to show the similarity to the stable condition. The scatter of normalized pressures was approximately the same ($\pm 3\frac{1}{2}$ percent at the injector face) as with the stable injector. Although the instability could be considered as an

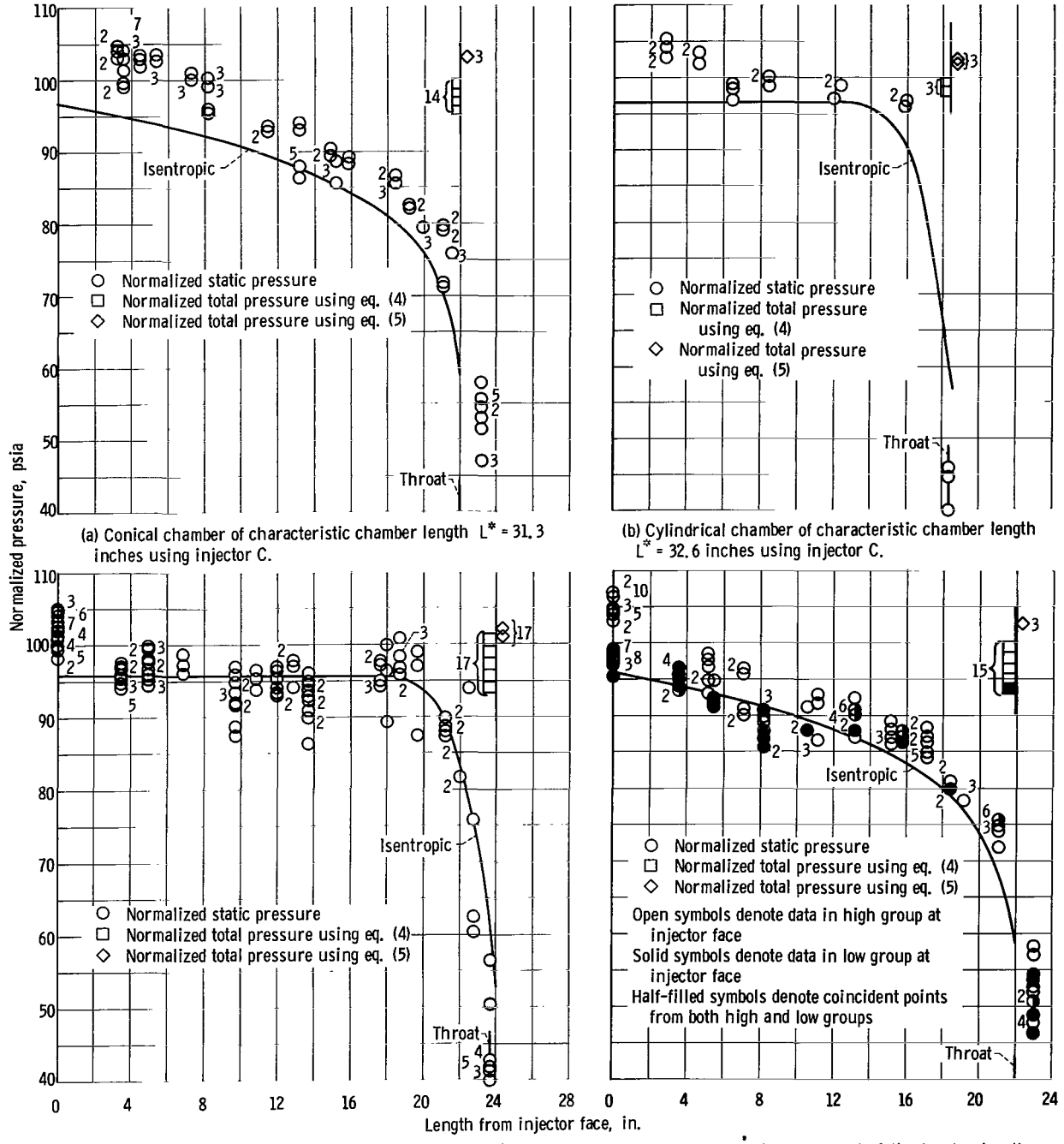

(a) Conical chamber of characteristic chamber length $L^* = 31.3$ inches using injector C.

(b) Cylindrical chamber of characteristic chamber length $L^* = 32.6$ inches using injector C.

(c) Cylindrical chamber of characteristic chamber length $L^* = 42.6$ inches using injector A.

(d) Conical chamber of characteristic chamber length $L^* = 31.3$ inches using injector A.

Figure 6. - Chamber pressure profiles at oxidant-to-fuel ratio of 2.0.

underlying influence on the pressures, the impulse data were not affected as evidenced by $P_{t,F}$. Although a comparison of the absolute value of throat total pressure as calculated using equations (4) and (5) does indicate a difference, the presence of the combustion instability made this comparison questionable.

Injector A exhibited unusual behavior in the conical chamber, however, as shown in figure 6(d). Injector face pressure appeared to scatter about two distinctly different levels, each level being a grouping $2\frac{1}{2}$ percent wide and separated by a band of 4 percent in which no data were recorded. The lower sets of data in figure 6(d) were shaded to distinguish between these two levels. Runs in which these two levels were recorded produced almost identical values of impulse. This anomaly was interpreted to mean that the injector was unstable at both conditions since the impulse was unchanged and that two different flow orientations were sustained in the screeching condition. The separation of pressures appeared to be maintained through the first 5 to 7 inches of the chamber but to a lesser degree.

With all the profiles, no location in the chamber appears to be suitable to produce data for total pressure calculation. At the subsonic nozzle entrance, for example, measured static pressures were several percent higher, notwithstanding the data scatter, than would be calculated for that area ratio using the thrust based total pressure. Variations in measured static pressure near the throat were particularly extreme with all chamber and injector combinations.

Injector B was not included in this discussion since it could not be run in the same chambers because of its slightly larger diameter. The results, however, were the same in that the scatter of chamber pressure readings was unacceptable for use in performance calculations. This injector did point out an additional problem of pressure distribution as the result perhaps of the spherical injector face and the baffles. Pressures at the center of the injector dome were approximately 3 percent higher than those measured at the edge of the spherical surface with an additional 5 percent reduction occurring at the first wall tap. The implication was clear that no single tap location at the injector end could be assumed to produce pressures that were representative of the effective injector face pressure for the purpose of performance calculations. This would certainly be true of injectors of unusual design and might also apply to flat faced injectors with coarse or nonuniform patterns.

The attempts to determine a total pressure profile using static pressures and streak photography were not pursued in light of the wide scatter of pressure shown in figure 6. Accurate velocity profiles were also difficult to obtain from the streak methods used.

The throat total probe made no contribution to this program although the results were encouraging enough to merit consideration in the future. The durability of the probe was demonstrated but reproducible data were not obtained from the instrumentation, even when parallel transducers were installed.

The experimental results coupled with the aforementioned problems of applying corrections to the various chamber pressure measurements dictated that thrust measurements from the low area ratio nozzles had to be used to obtain c* performance.

Resolved Calculation Procedure

When the large area ratio nozzles were attached to the chambers, no satisfactory measurements were available for c* and $C_{F,v}$ calculation since chamber pressures were not reliable and thrust coefficient could not be predicted. Therefore, a procedure was resolved that consisted of "calibrating" the injector-chamber combination with a low area ratio nozzle (ϵ = 1.30 and 1.42) to determine characteristic velocity efficiency η_{c*} as a function of mixture ratio.

The equation used for this calculation was

$$\eta_{c*} = \frac{\eta_{I_v}}{\eta_{C_{F,v}}} = \frac{\eta_{I_v}}{0.980}\Bigg|_{\epsilon = 1.30,\ 1.42} \tag{6}$$

where

$$\eta_{I_v} = \frac{\frac{F_v}{\dot{w}}}{I_{v,T}} \tag{7}$$

The high area ratio nozzle performance could then be calculated from high area ratio impulse measurements at the measured mixture ratio using the c* calibration curve and the following equation:

$$C_{F,v} = \frac{I_v g}{\eta_{c*} \times c^*_T}\Bigg|_{\epsilon = 60,\ 40} \tag{8}$$

These equations apply, of course, whether absolute values or efficiencies are used since all values subscripted with T are for one-dimensional, isentropic, equilibrium flow. Figure 7 is a flow chart showing the steps in this calculation procedure. The key to this method was the assumption that the accuracy of the analytically determined thrust coefficient of the low area ratio nozzle (ϵ = 1.30 and 1.42) was better than experimentally measured chamber pressures. The resulting procedure needed only vacuum thrust and

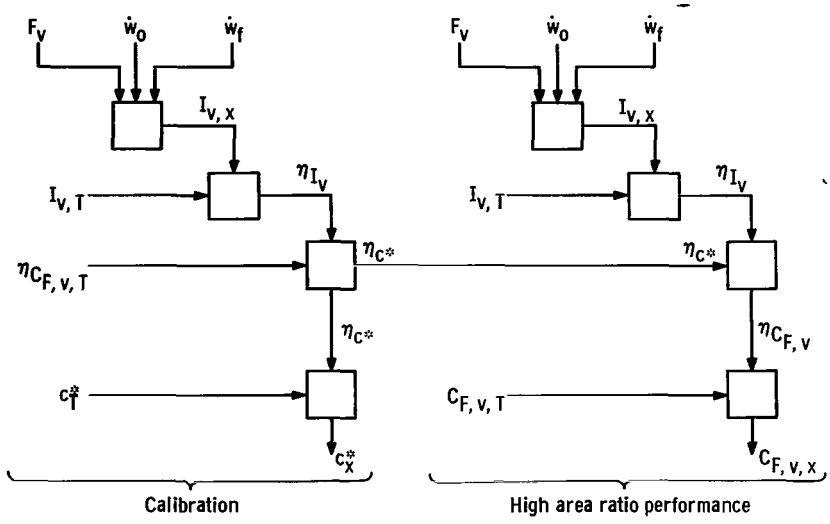

Figure 7. - Flow chart showing method of calculation.

flow measurements, but no chamber pressures, to obtain all performance parameters for both low and high area ratio engines. This calculation procedure will be used exclusively for all data discussed in the remainder of this report.

Characteristic Velocity Studies

The c* calibration curves were the end product of a thorough evaluation of the three primary injectors over a mixture ratio range of 1.4 to 2.2 in combustion chambers of several lengths and geometries. A discussion of the basic injector-chamber data follows.

Injector evaluation. - The results of the low area ratio testing in which injectors A, B, and C were run in various chambers are presented in figure 8. This figure also served as the calibration curves for the various injector-chamber combinations.

Injector A was run through many configurations before suitable instrumentation became available, which showed that the combustion was consistently unstable in the second (3960-cps) or third (5450-cps) tangential modes of acoustical instability. Initial monitoring to detect "screech" had been attempted with a microphone in the test cell, but analysis of the recorded tapes gave no indication that the problem existed. The η_{c^*} performance was 97.1 percent at all mixture ratios and with all chamber geometries, undoubtedly because of the high-frequency instability. Note that, in spite of the instability, data from 71 runs over the mixture ratio range fell into a band that was ±1 percent wide, evidence of the repeatability of thrust and flow measurements. Although the value of an unstable injector was questionable, the performance results are included because of some interesting observations made when this injector was run with the large area ratio nozzles; these will be discussed later.

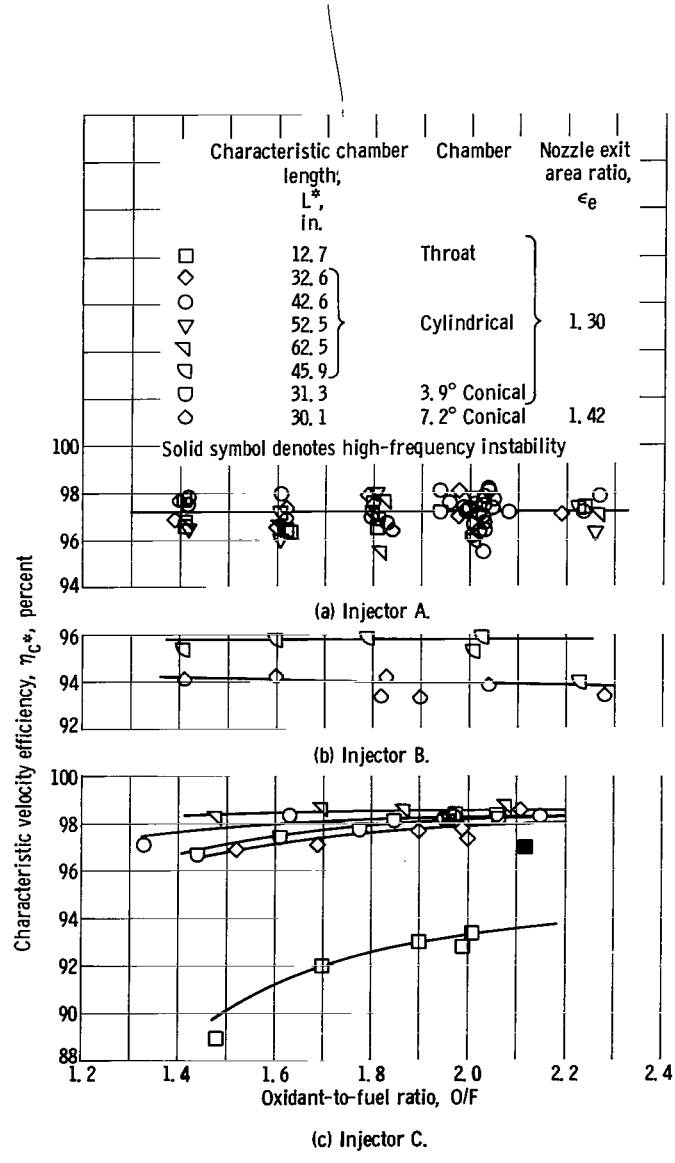

Figure 8. - Injector performance evaluation.

The η_{c^*} performance of injector B was obtained with only two chambers since this injector was slightly larger in diameter and did not fit the standard chambers. The c* efficiencies with injector B were 1 to 3 percent below the data from injector A, probably the result of the assignment of 6 percent of the fuel area to film cooling. In the transtage conical chamber of $L^* = 30.1$ inches, the c* efficiency was only 93.9 percent at $O/F = 2.0$ but, since this injector was stable, it was more sensitive to chamber geometry effects and increasing L^* to 45.9 inches raised η_{c^*} to 95.8 percent.

The evaluation of injector C proved that it was clearly the best injector to produce dependable results for the large area ratio nozzle tests because of high performance and stable combustion. For all chambers except the throat section ($L^* = 12.7$ in.), the c* efficiencies were about 98.0 percent or greater at $O/F = 2.0$. As was the case previously, η_{c^*} calculated from thrust and flow rate (eq. (4)) resulted in very little data scatter. At $O/F = 2.0$, injector C was 1 percent better than injector A and 4 percent better than injector B in chambers of nominal L^* of 30 to 32 inches. Flush mounted high-frequency transducers showed injector C to be stable for 54 of 55 runs during the program. Note that the one instance of instability improved performance for the chamber having $L^* = 12.7$ inches.

Although the performance of the three injectors were directly compared in this discussion, the determination of which injector was best depends on the application. As mentioned, injector C best met the needs of this program but it undoubtably would not have complied with the dynamic stability criteria (bombing) and ablative chamber compatibility requirements that governed the design of injector B.

Combustion chamber effects. - To separate the geometrical effects of the various combustion chambers, the data for mixture ratios of 2.0 and 1.6 from figure 8 are also plotted against characteristic length L^* in figure 9. Since injector C was of primary interest, the data for injectors A and B were omitted for clarity and only the curve fit is shown for these injectors. For a mixture ratio of 2.0, the choice of L^* near 31.3 inches for the Apollo SPS appears near an optimum since less than 1 percent improvement can be obtained by doubling the chamber characteristic length with the high-performing injector C. At $O/F = 1.6$, which is near the mixture ratio for maximum theoretical c*,

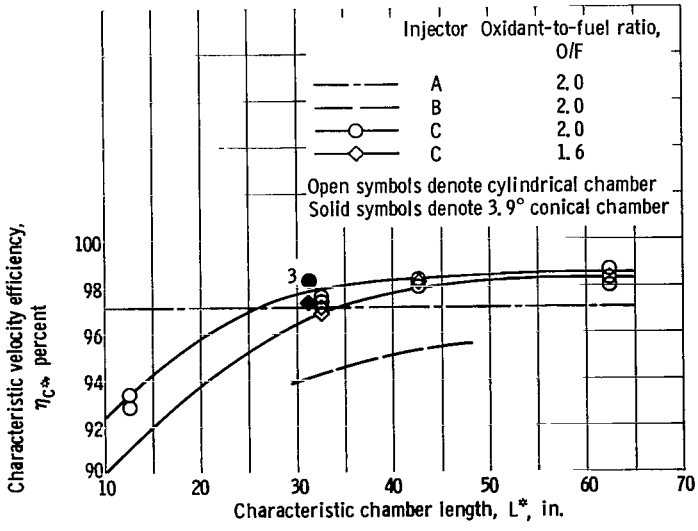

Figure 9. - Effect of chamber on characteristic velocity efficiency.

problems of mixing make the attainment of high efficiency more difficult; therefore, c* efficiency is more sensitive to chamber characteristic length for this mixture ratio. When the performance of conical chambers is compared to that of cylindrical chambers with the same L^*, essentially no difference was observed with the 3.9° cone. Reference to figure 8 shows this comparison more clearly. With the 7.2° cone, the results were inconclusive but it would appear that any differences would be small.

The dominant effect of combustion instability on performance was shown very dramatically in figure 9 with injector A. This screeching injector experienced no dropoff in performance from the maximum c* efficiency of 97.1 percent even when operated at $L^* = 12.7$ inches, which was essentially just a throat section with a 1-inch-long chamber.

Effects of combustion instability. - Before the discussion of the combustion chamber results is terminated, the possible effects of instability on processes other than combustion should be considered. The instability with injector A was first detected conclusively through the use of streak photography. A sample of the streak photography is presented in figure 10 to show primarily the sensitivity of this method of monitoring combustion instability. The frequency and mode of instability are readily discernible, but amplitude and wave form require more sophisticated instrumentation. When compared to the high-frequency transducer, the light intensity variation of the instability was found to

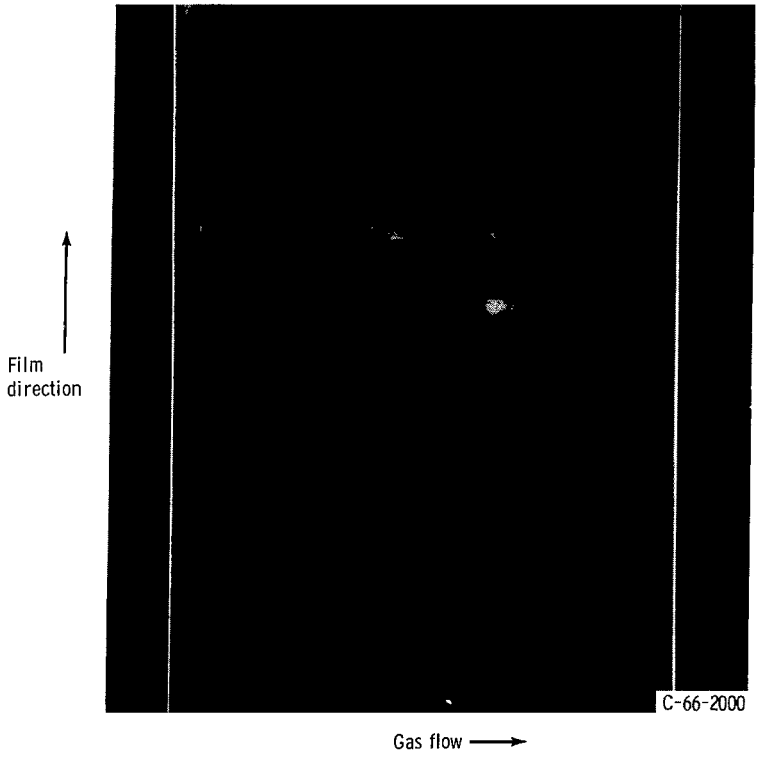

Figure 10. - Streak photograph of 3960-cps tangential mode of combustion instability with injection A.

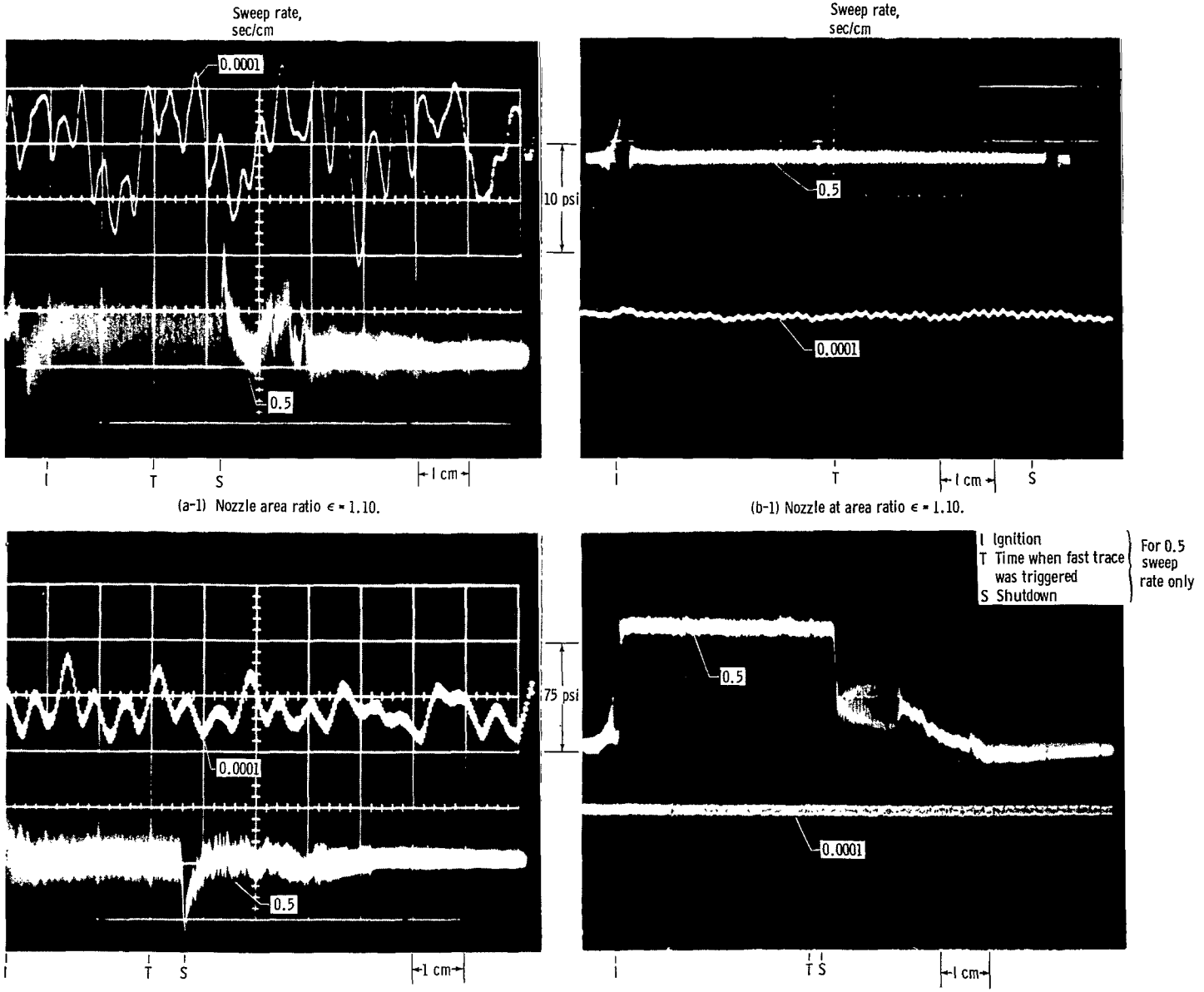

Figure 11. - Transmission of combustion instability into supersonic portion of nozzle.

represent ±20-pound-per-square-inch oscillation from 100-pound-per-square-inch mean value.

As mentioned previously, this instability did not appear on recordings made through a microphone located in the test cell. Since injector A had been run in the large area ratio nozzles before it was determined to be unstable, the validity of impulse and thrust coefficient was certainly to be questioned. In order to provide additional information on this problem, high-frequency instrumentation was flush mounted in the supersonic portion of the nozzle at an area ratio of 1.10 as well as in the combustion chamber. Figure 11(a-2) shows the output of the transducer mounted in the combustion chamber using injector A where the mode of instability was the second tangential with an amplitude of ±20 percent of chamber pressure. Figure 11(a-1) shows the oscillations have propagated through the throat and at an area ratio of 1.1 still appear as ±20 percent of the local static pressure. This fluctuation of pressure and, consequently, all gas properties had no measurable effect on the impulse with the area-ratio-1.3 nozzle.

The high-frequency transducer output using injector C was included in the photographs of figure 11(b) for comparison when stable combustion existed. The chamber pickup in this case only shows the static pressure level also. With injector C the combustion noise was less than the noise level of this particular instrument system.

Vacuum Specific Impulse with High Area Ratio Nozzles

This portion of the program was intended to demonstrate the maximum attainable vacuum impulse capability of complete engines using the propellant combination of N_2O_4 and the 50-50 blend. In all cases, the impulse was computed using measured thrust plus the vacuum correction for the pressure acting on the external surface of the engine. No additional factors were involved.

Area-ratio-60, 15^o conical nozzle. - The delivered vacuum specific impulse with the area-ratio-60, 15^o conical nozzle is shown in figure 12(a) with the 3.9^o conical combustion chamber. Injectors A and C were run with this engine. At a mixture ratio of 2.0, the engine produced 319.5 seconds of vacuum specific impulse with injector C, which was previously documented at 98.2 percent c* efficiency. Operating at a mixture ratio of 1.6 reduced the impulse to 318.3 seconds, while a peak of about 320.5 seconds was probably available at O/F = 1.8. Note that the impulse difference at a mixture ratio of 2.0 for injectors A and C is 3 seconds or 1 percent, which is identical to the difference in characteristic velocity efficiency of these two injectors.

Additional comparisons using the 15^o conical, area-ratio-60 nozzle are made in figure 12(b) for cylindrical chambers with injectors B (L^* = 45.9 in.) and C (L^* = 42.6 in.). In this slightly longer chamber the c* calibration of injector C indicated a per-

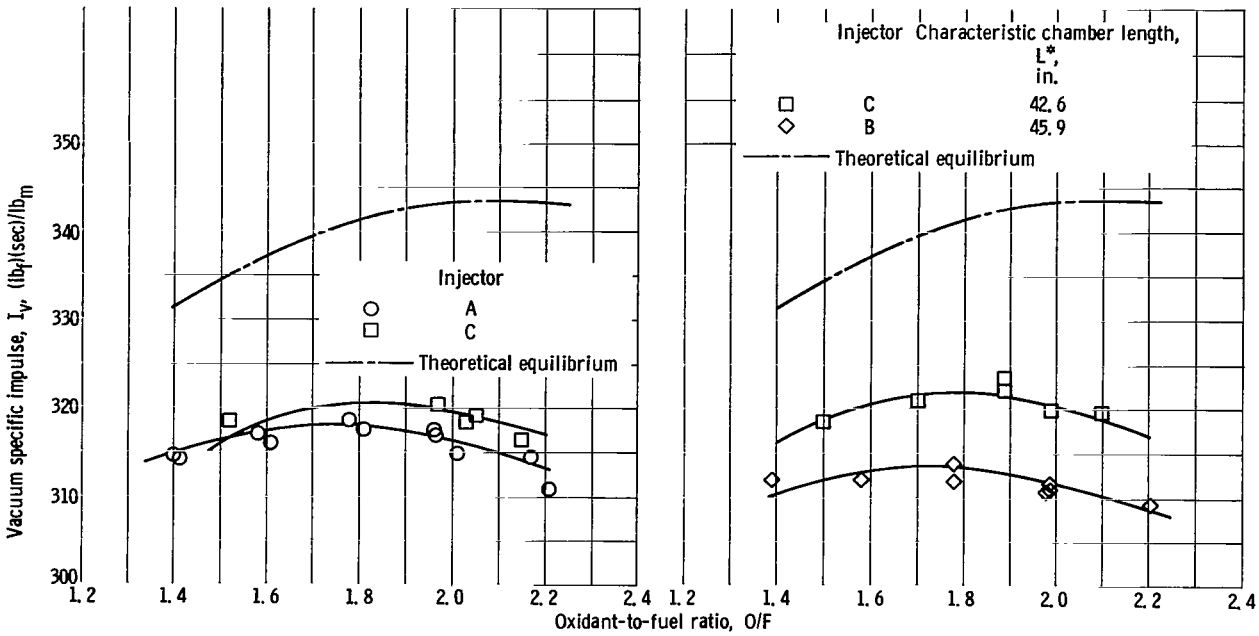

(a) 3.9° Conical chamber of characteristic chamber length $L^* = 31.3$ inches.

(b) Cylindrical chambers of characteristic chamber length $L^* = 42.6$ and 45.9 inches.

Figure 12. - Performance of engine with area-ratio-60, 15° conical nozzle.

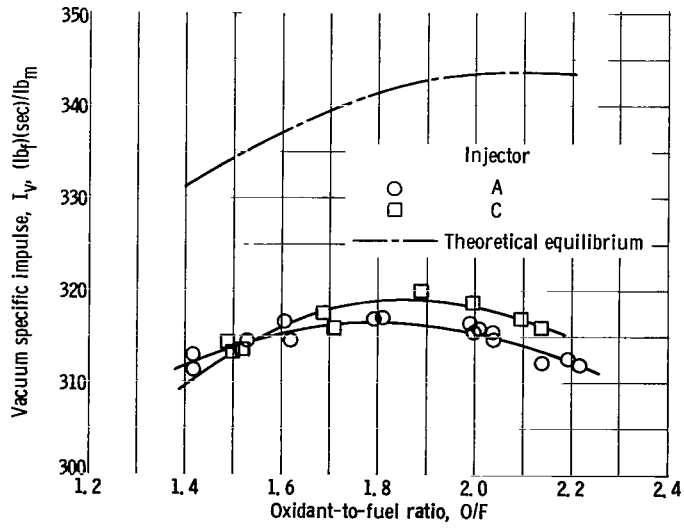

Figure 13. - Performance of scaled Service Module Propulsion System engine (67.9 percent area-ratio-60 contour nozzle with 3.9° conical chamber of characteristic chamber length $L^* = 31.3$ in.).

formance improvement over the chambers for which $L^* = 32$ inches and resulted in the maximum delivered impulse during the program of about 322.5 seconds at $O/F = 1.9$. Injector B produced a high of 313.5 seconds at $O/F = 1.7$ with this configuration.

Area-ratio-60, Service Module Propulsion System contour nozzle. - The delivered vacuum specific impulse of the 40 percent scale version of the Apollo Service Module Propulsion System with injectors A and C is presented in figure 13. As described earlier, this engine consisted of a 3.9° conical chamber of $L^* = 31.3$ inches and an area-ratio-60 nozzle contoured to 67.9 percent of the length of a 15° cone. With injector C this configuration showed an impulse capa-

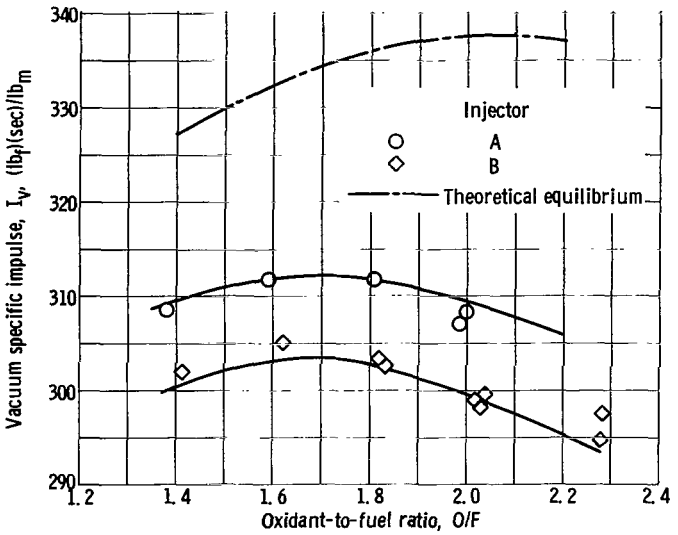

Figure 14. - Performance of Titan transtage engine (66.3 percent area-ratio-40 contour nozzle with 7.2° conical chamber of characteristic chamber length $L^* = 30.1$ in.).

bility of 318.0 seconds at the Apollo design O/F = 2.0, with a peak of 319.0 seconds available at O/F = 1.9. At a mixture ratio of 1.6, the delivered impulse was reduced to 316.0 seconds because of the c* efficiency profile of injector C. The difference in impulse between the engines using injectors A and C was again identical to the trends recorded during the injector calibration tests.

Area-ratio-40, Titan transtage contour nozzle. - The full-scale version of the Titan transtage engine was run with injectors A and B; these results are presented in figure 14. The transtage engine consisted of a 7.2° conical chamber of $L^* = 30.1$ inches and an area-ratio-40 nozzle contoured to 66.3 percent of the length of a 15° cone. At O/F = 2.0, delivered performance with injectors A and B was 308.5 and 300.0 seconds impulse, respectively. However, the data obtained with injector B appears to be about 0.5 percent high at mixture ratios other than O/F = 1.8 and 2.0. The performance of this area-ratio-40 nozzle tended to maximize at slightly lower mixture ratios than that of the area-ratio-60 nozzles with a peak at O/F = 1.7 being about 3.5 seconds higher than O/F = 2.0.

Vacuum Thrust Coefficients of High Area Ratio Nozzles

One of the most important considerations in determining the performance capability of this propellant combination is the nozzle expansion process and the degree to which this approaches chemical equilibrium. With rocket engine data, the nozzle performance is described by the thrust coefficient, which does not include the various c* deficiencies. Therefore, all tests with a given nozzle should be comparable regardless of the injector performance, provided the injector does not introduce peculiarities because of very low c* efficiency or extreme distribution of gas properties. For the next series of figures, the large area ratio impulse data were combined with the respective c* calibrations, according to the procedure previously resolved, to obtain the delivered vacuum thrust coefficients for the three nozzles.

Area-ratio-60, 15° conical nozzle. - This nozzle, chosen as a standard for com-

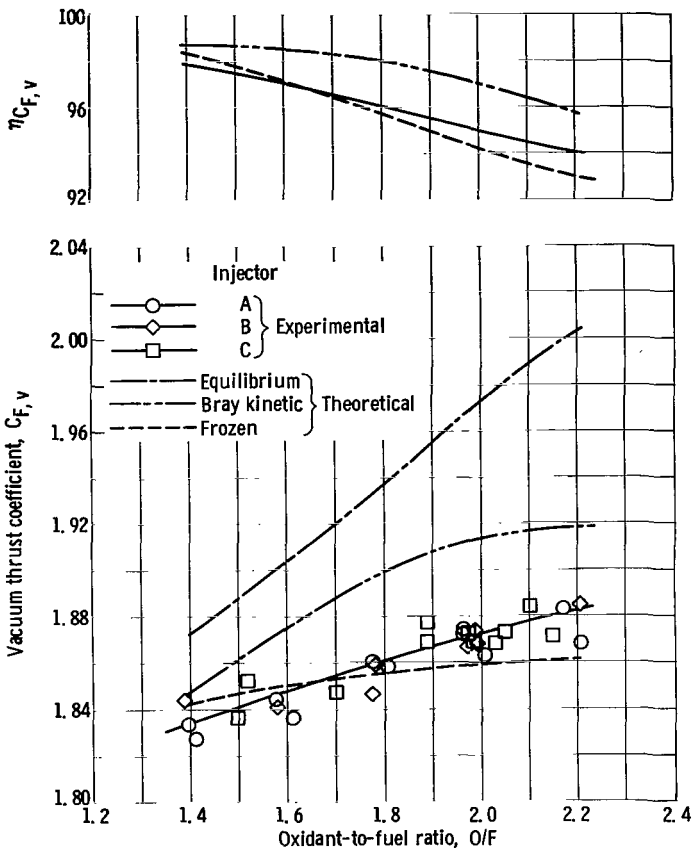

Figure 15. - Performance of area-ratio-60, 15° conical nozzle.

parison, was run with four different injector-chamber combinations including all three injectors. Vacuum thrust coefficients calculated from all the runs are presented in figure 15. This nozzle produced the highest thrust coefficients of the three nozzles tested, with a value of 1.872 attained at O/F = 2.0. This corresponds to 95 percent of the one-dimensional theoretical equilibrium value. At lower mixture ratios higher nozzle efficiencies were recorded, but the absolute coefficient was considerably less. Operating at a mixture ratio of 1.6 would result in about a 1.3 percent reduction in absolute thrust coefficient from the value at O/F = 2.0. Of particular interest is the fact that all of the 30 data points fell at random within ±0.5 percent of the best line through all the data, even though the c* efficiencies of the different chamber-injector combinations varied from 98.2 to 95.5 percent and included both stable and screeching combustion. Precision of this order substantiated the method of calculating throat total pressure, c*, and C_F from the thrust and flow measurements as previously described since the use of chamber pressure measurements would make this band about 7 percent wide.

Area-ratio-60, Service Module Propulsion System contour nozzle. - The scaled Apollo SPS nozzle thrust coefficients were obtained from engine data using injectors A and C, both in the Apollo chamber, and are shown in figure 16. At a mixture ratio of 2.0, this area-ratio-60 contoured nozzle produced a value of 1.865, equivalent to 94.6 percent of equilibrium. Shifting the value of O/F to 1.6 reduced absolute nozzle performance by 1.7 percent to 1.834. The delivered thrust coefficients of the contoured nozzle were 0.5 to 1 percent lower than the conical nozzle. Again, the precision was excellent with 23 of 24 points falling within ±0.4 percent of the best line. As with the conical nozzle, the fluctuation of gas properties caused by the unstable injector A did not alter the nozzle performance.

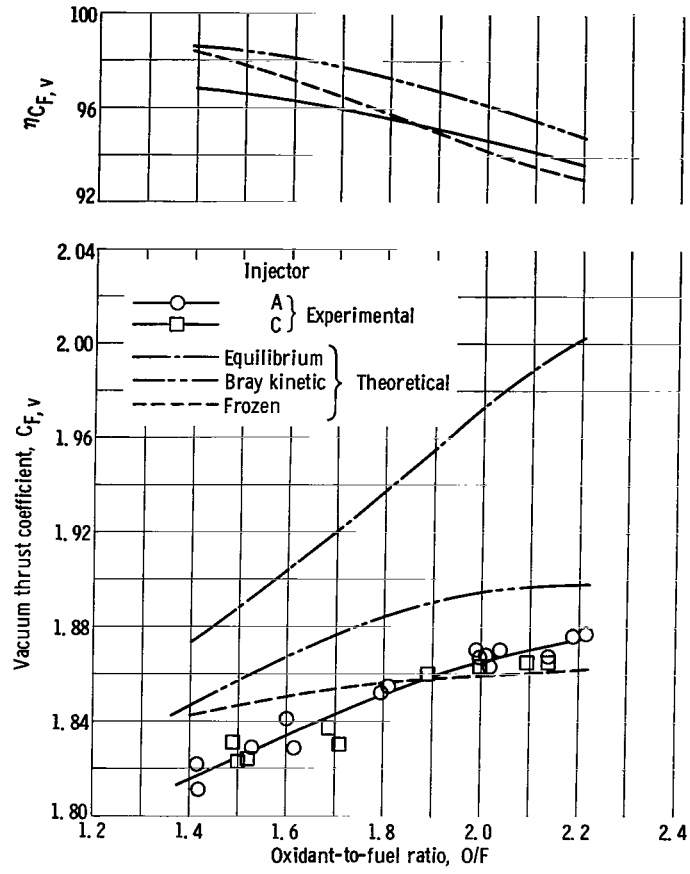

Figure 16. - Performance of area-ratio-60, scaled Service Module Propulsion System contour nozzle.

Area-ratio-40, Titan transtage contour nozzle. - Vacuum thrust coefficients for the transtage contoured nozzle were obtained from engine data using injectors A and B in the transtage chamber, and are presented in figure 17. At O/F = 2.0, the average value of thrust coefficient was 1.832 corresponding to 94.4 percent of theoretical equilibrium. Experimentally, the sensitivity of thrust coefficient to mixture ratio was less for this nozzle than for the area-ratio-60 nozzles, and a shift in operating point from O/F = 2.0 to 1.6 reduced nozzle performance only 1.0 percent. Although a large number of data points were not obtained, the precision still seems reasonable with 11 of the 14 points falling within ±0.5 percent of the best line. The nozzle performance does not appear to be significantly influenced by chamber performance even though the c* efficiencies of the two injector-chamber configurations used with this nozzle ranged from 94 to 97.2 percent. It should be noted, however, that the limited data available for the evaluation of injector B (fig. 8, p. 24) did not define the c* calibration curve as specifically as the other injectors. It was possible to alter the calibration curve fairing for injector B in such a manner that the calculation of $C_{F,v}$ with the area-ratio-40 contour nozzle would

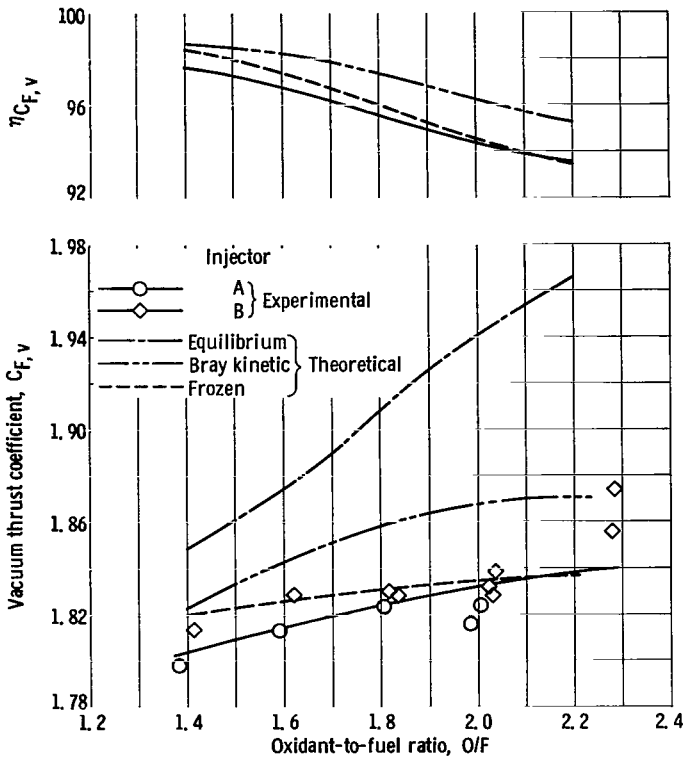

Figure 17. - Performance of area-ratio-40, Titan transtage contour nozzle.

indicate an effect of c* on $C_{F,v}$. The result would indicate slightly higher (but less than 0.5 percent) $C_{F,v}$ with the lower η_{c*} of injector B as compared to data obtained with injector A. No apparent influence existed, however, at O/F = 1.8 and 2.0. This alternate fairing of injector B calibration data was not chosen since the effect was not definite with the area-ratio-40 contour nozzle and almost insignificant when reviewing the results with the area-ratio-60, 15° conical nozzle.

Correlations with Analytical Models

Not until the discussion is limited to just nozzle performance can the experimental results be compared to equilibrium, frozen, or some intermediate expansion model. In the case of figures 15 to 17, the thrust coefficient, by definition, further restricted the comparison to the supersonic flow field. Identification of the major areas of difference between the experimental and one-dimensional theoretical equilibrium was attempted using two computer programs. Losses due to nonequilibrium expansion were approximated with a program utilizing Bray's criterion of sudden freezing. This program was developed at Lewis and is described in reference 8. Aerodynamic or flow losses were evaluated using a method of characteristics program that included friction calculations.

The Bray criterion calculations for the two area-ratio-60 nozzles were also included in figures 15 and 16. The experimental data were more nearly parallel to the theoretical Bray kinetic curve than either the equilibrium or the frozen expansion possibilities. Therefore the influence of reaction kinetics in the expansion process was indicated. A slight sensitivity of the kinetics to nozzle contour was also indicated since the scaled SPS nozzle did not develop as high a thrust coefficient as the 15° conical; this was predicted by the kinetic calculations.

To indicate what the ultimate capability of the complete Apollo SPS engine might be and to point out the distribution of the losses, the thrust coefficient data of figure 16 were

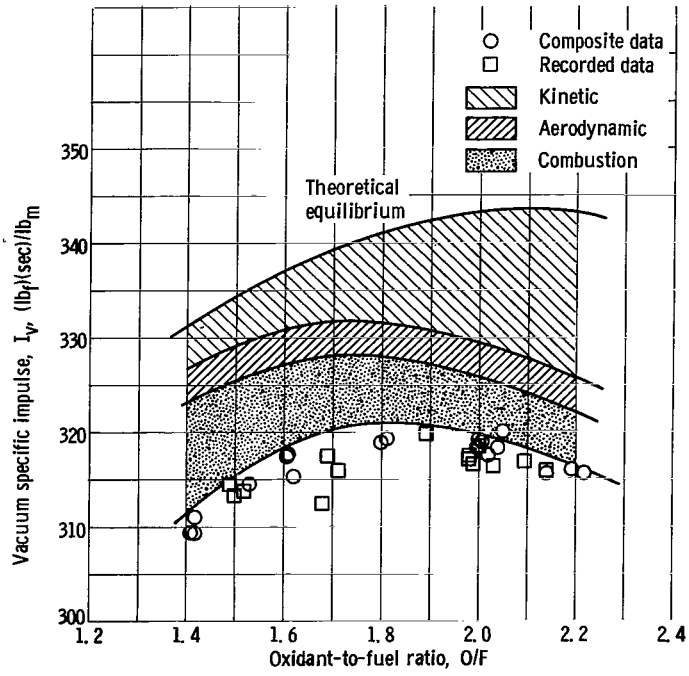

Figure 18. - Effect of mixture ratio on distribution of engine losses for scaled Service Module Propulsion System engine.

replotted in figure 18 using a scale factor to express the thrust coefficient in terms of vacuum impulse. This scale factor was c*/g using the characteristic velocity for injector C in the 3.9^{o} conical chamber. As a result, the points that originated with injector C are actual recorded data, but the remainder are experimentally derived composites. The solid lines in figure 18 represent successive products of the analytical kinetic efficiency, analytical aerodynamic efficiency, and experimental combustion efficiency. Although these three processes are certainly interdependent, the result would be very tedious to compute and also subject to argument. However, the ability to perform these calculations has been developed and is described in reference 9.

The three major areas of deficiency are seen in figure 18 to account for virtually all the difference between the experimentally derived data and the one-dimensional theoretical equilibrium. At the Apollo design mixture ratio of 2.0, an impulse of 316.0 to 319.0 seconds would be very difficult to exceed since these data were delivered using a 98 percent c* injector-chamber configuration. Practical problems such as ablative chamber compatibility and acoustical damping devices would probably force a compromise to a lower impulse. Although, with this particular injector, a shift to an O/F of 1.6 would degrade performance by about 2 seconds, any injector that could offset the 1.7 percent drop in C_F by a corresponding increase in c* would benefit from the shift to the lower combustion temperature environment.

Figure 18 also points out that the kinetic losses of 4 percent at a mixture ratio of 2.0 were considerably more significant than the aerodynamic losses of 1 percent whereas at lower mixture ratios the kinetic losses and aerodynamic losses were of the same order of magnitude.

An interesting approach to the use of these correlation schemes was found by looking at the computer outputs during the expansion through the nozzle. In figure 19, the various efficiencies were again compounded to obtain the available impulse at any point in the SPS contour nozzle. The kinetic losses that started at an area ratio of 1.3 became more significant as area ratio increased, since the unavailable energy of recombination was

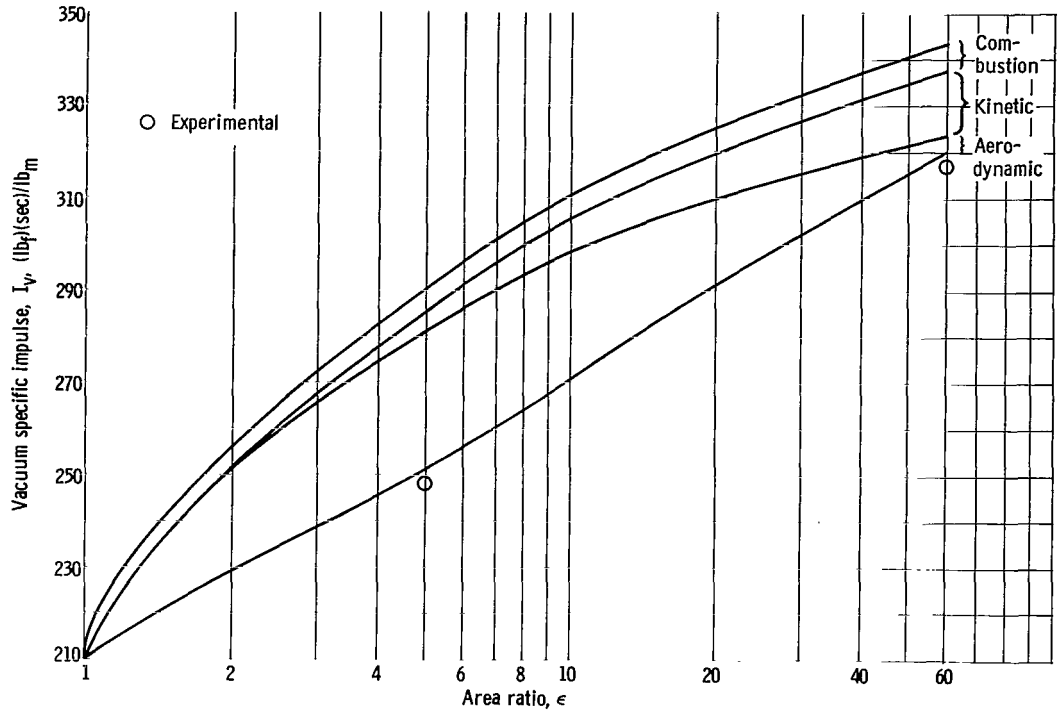

Figure 19. - Distribution of losses during nozzle expansion for scaled Service Module Propulsion System contour. Oxidant-to-fuel ratio O/F = 2.0; combustion chamber pressure P_c = 100 pounds per square inch absolute.

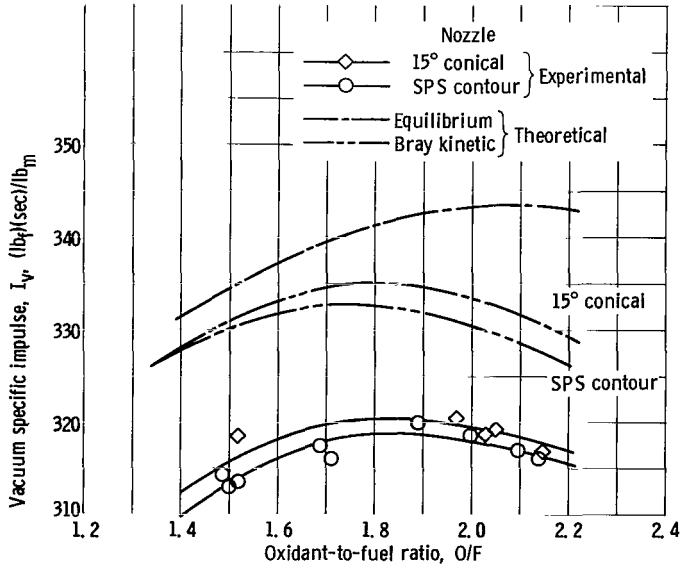

Figure 20. - Comparison of engine capabilities with injector C, 3.9° conical chamber, and two area-ratio-60 nozzles.

becoming more significant. The aerodynamic performance was very poor within the nozzle because of the high flow angles and was very good at an area ratio of 60 since that was the design point for the contour. The two data points represent delivered experimental data at area ratios of 60 and 5. The latter data point was obtained during the catalytic injection tests with the nozzle contour terminated at an assembly joint. The two experimental points show less than 1 percent is unaccounted for with this correlation method at both large and small area ratios.

Finally, a comparison of the two area-ratio-60 nozzles using injector C is made in figure 20. This

shows that an indiscriminate increase in nozzle length to improve chemical kinetic performance does not provide the needed improvement in engine performance. The theoretical kinetic potential difference between the SPS contour and the 15^{o} conical nozzles was about 1 percent at O/F = 2.0 as indicated by the two Bray curves. Although it appeared experimentally that some of this potential was realized with the conical nozzle, it would be problematical for a mission analysis to show that this 0.5 to 1 percent improvement potential in impulse would offset the greater nozzle length of the 15^{o} conic.

Potential for Performance Improvement

Any search for area that might offer some potential for performance improvement within the engine would be directed toward the injector, combustion chamber, or nozzle.

Injector improvements were not investigated because of the specific nature of the design requirements of a flight injector in complying with stability criteria and chamber compatibility for a specific thrust level. The high performance and stable combustion of injector C adequately filled the needs of the program.

The possibility for improvement of performance from chamber modifications was investigated to some extent experimentally with the conclusion that a performance advantage was possible using additional chamber length, particularly if the injector were poor to begin with (fig. 9, p. 25).

The nonequilibrium effects in the nozzle, however, did appear to be an area worthy of investigation, since the losses attributable to kinetic effects were so large. The approach taken was to find means to extend the region of equilibrium flow. The two methods attempted were to (1) reshape the nozzle contour to maintain conditions favorable to continue recombination and (2) inject a third fluid to act as a catalyst to accelerate the rate of recombination.

The first method was attempted on the computer using the Bray kinetic program and its various options. The potential improvement attributable to kinetics was formulated by calculating the one-dimensional impulse available from an area-ratio-60 nozzle as a function of the area ratio at which "sudden freezing" took place. This initial step assumed, hypothetically, that the location of the freezing point could be varied or controlled. Next, the flow angle necessary to maintain equilibrium conditions was determined for several freezing area ratios, and the results of these two calculation procedures were used to define the first portion of several contour nozzles, which were then evaluated aerodynamically with the method of characteristics. In all cases evaluated, shocks were predicted for this controlled section of the nozzle and further attempts were abandoned. This recontouring approach might prove successful for a system such as hydrogen fluorine where greater sensitivity to freezing area ratio is possible, thereby permitting more liberal aerodynamic designs.

The second method was attempted experimentally with no encouraging results. Benzene and ethylene were chosen from reference 10 as potential catalysts for the $H+H \rightleftharpoons H_2$ recombination reaction, with flow rates up to 1 percent of the total flow considered adequate. The catalytic injection system consisted of four spray bars located 2 inches upstream of the nozzle throat and projecting out from the chamber walls toward the centerline. Numerous hole patterns varying in number from four to twenty were tested in an attempt to obtain good distribution through the mainstream. Efficiency of the distribution was monitored with a color movie camera aimed upstream from the engine exit. During a typical run, the catalyst was injected from the start of a 6-second firing and terminated after 3 seconds. Any performance shifts because of catalytic injection would appear as a step change at the cutoff point in the run. With ethylene, the impulse increased after the termination of the third fluid indicating no catalysis had taken place and that the performance decrement was due to the expansion of the higher molecular weight hydrocarbon gas. No performance change was observed using benzene, giving rise to the possibility that sufficient catalysis took place to offset the expansion of the very high molecular weight addition. The lack of any positive performance improvement coupled with the difficulty of obtaining satisfactory distribution of the catalyst led to the termination of this approach to performance improvement.

SUMMARY OF RESULTS

An experimental investigation of the performance of nitrogen tetroxide and a blend of 50 percent hydrazine and 50 percent unsymmetrical dimethyl hydrazine was conducted in rocket engines at a 9000-pound thrust level and a chamber pressure of 100 pounds per square inch. Two contoured nozzles with area ratios of 60 and 40 plus a 15° conical nozzle with an area ratio of 60 were operated over an oxidant-to-fuel ratio O/F ranging from 1.4 to 2.2. The results were summarized as follows:

1. At a mixture ratio of 2.0 with an area-ratio-60, 15° conical nozzle, the maximum vacuum impulse was about 320 seconds. However, practical limitations on chamber and nozzle length as typified by the Apollo Service Module Propulsion System (SPS) contoured nozzle reduced this value to approximately 318 seconds. At an area ratio of 40, the Titan transtage contoured nozzle delivered 308 seconds at O/F = 2.0 although this engine was not tested with the highest performing injector.

2. The most simple assured method to determine reliable characteristic velocity c* performance from an injector-chamber combination involved impulse measurements with a low area ratio nozzle. Pressures measured in the chamber were not acceptable for the determination of performance.

3. Of the three injectors used, the best produced a c* efficiency of 98 percent at

O/F = 2.0 in chambers having a characteristic chamber length L^* = 32 inches. Increasing chamber length to L^* = 62.5 inches with this injector improved performance about 1/2 percent. Performance at lower mixture ratios and with poorer injectors was more sensitive to chamber length. Performance of one injector that was unstable was completely independent of chamber length. No difference in c* performance was observed when the results obtained using a 3.9° conical chamber were compared to the results using a cylindrical chamber of the same L^* with the same injector.

4. The vacuum thrust coefficients for an area ratio of 60 and O/F = 2.0 were 1.872 and 1.865 seconds for the 15° conical and SPS contour nozzles, respectively. The differences were attributed to the nonequilibrium kinetics of the recombination process during expansion. At an area ratio of 40, the transtage contoured nozzle delivered a value of 1.832 seconds at O/F = 2.0. Experimentally it was observed that essentially all thrust coefficients were within ±0.5 percent of the nominal value regardless of c* efficiency, which varied from 98 to 94 percent with the three injectors. The tight band of thrust coefficient data also included results from an injector that produced high-frequency combustion instability.

5. The experimental thrust coefficients were correlated analytically, using the method of characteristics to evaluate aerodynamic performance and the Bray criteria to evaluate nonequilibrium performance. Essentially all of the difference between theoretical equilibrium and experimental data were accounted for in this manner.

6. Efforts were made to determine if nozzle performance could be improved over conventional nozzle designs by promoting equilibrium flow to higher area ratios. Analytically, this was attempted by recontouring the nozzle based on kinetic considerations, but these contours were not shock free when aerodynamically evaluated so this approach was abandoned. Experimentally, the injection of a third fluid to act as a catalyst was attempted but no positive advantage was realized using benzene and ethylene.

7. The feasibility of a total pressure probe in the throat of a rocket engine was demonstrated although no significant data were obtained.

Lewis Research Center,
National Aeronautics and Space Administration,
Cleveland, Ohio, April 18, 1966,
104-31-02-01-22.

APPENDIX A

SYMBOLS

A	area, sq in.
C_F	thrust coefficient (experimental unless otherwise specified)
c*	characteristic velocity (experimental unless otherwise specified), ft/sec
D	diameter, in.
F	thrust, lb
g	gravitational conversion factor, 32.174 ft/sec^2
H_f	enthalpy of formation, cal/mole
I	specific impulse (experimental unless otherwise specified), $(lb_f)(sec)/lb_m$
L	length, in.
L^*	characteristic chamber length (L^* = chamber volume/throat area), in.
O/F	oxidant-to-fuel ratio
P	total pressure, psia
p	static pressure, psia
p'	normalized pressure, psia
R	radius of curvature, in.
V	average propellant injection velocity, ft/sec
$\dot{w}$	propellant mass flow (total unless otherwise specified)
X	nozzle coordinate (axial distance from throat), in.
Y	nozzle coordinate (radial distance from centerline), in.
α	nozzle wall angle, deg
ϵ	area ratio
η	efficiency

Subscripts:

a	ambient conditions
c	combustion chamber
e	nozzle exit
F	thrust
f	fuel
i	injector face
m	measured
max	maximum
n	subsonic nozzle entrance
o	oxidizer
T	theoretical equilibrium, one dimensional
t	nozzle throat
x	experimental
v	vacuum conditions

APPENDIX B

THERMOCHEMICAL CALCULATIONS

The theoretical calculations were made at Lewis Research Center using the computer program described in reference 11. Calculations were based on the usual assumptions of perfect gas law, adiabatic combustion at constant pressure (nozzle inlet total pressure), isentropic expansion, no friction, homogeneous mixing, and one-dimensional flow.

All propellants were assumed to originate from the liquid state at atmospheric pressure and 298.1° K. The enthalpy of formation in calories per mole for each component is given in table VI. The value for N_2O_4 in table VI assumes no dissociation to NO_2 at these conditions. If the initial condition of the oxidizer were assumed to be an equilibrium mixture of $N_2O_4 \rightleftarrows 2NO_2$ at the boiling point of 294° K for atmospheric pressure, the heat of formation would have been -4631 calories per mole. The resulting influence on theoretical performance is given in table VII for comparison.

TABLE VI. - ENTHALPY OF FORMATION USED IN THEORETICAL CALCULATIONS

Propellant	Enthalpy of formation, H_f, cal/mole
N_2H_4	12 050.0
$N_2H_2(CH_3)_2$	12 734.8
N_2O_4	-6 873.0

TABLE VII. - INFLUENCE OF ENTHALPY OF FORMATION ON THEORETICAL PERFORMANCE

	Enthalpy of formation, H_f, cal/mole		Increase in theoretical performance, percent
	-6873.0	-4631.0	
Characteristic velocity, c*, ft/sec	5597	5612	0.3
Vacuum specific impulse, I_v, $(lb_f)(sec)/lb_m$	343.5	344.8	.4
Vacuum thrust coefficient, $C_{F,v}$	1.974	1.977	.1

REFERENCES

1. Jones, William L.; Aukerman, Carl A.; and Gibb, John W.: Experimental Performance of a Hydrogen-Fluorine Rocket Engine at Several Chamber Pressures and Exhaust-Nozzle Expansion Area Ratios. NASA TM X-387, 1960.

2. Aukerman, Carl A.; and Church, Bruce E.: Experimental Hydrogen-Fluorine Rocket Performance at Low Pressures and High Area Ratios. NASA TM X-724, 1963.

3. Hammock, W. R.; and Barton, D. L.: Results of Simulated Altitude Testing of UTC Subscale Ablatively Cooled Liquid-Propellant Rocket Engines for the Apollo Spacecraft. (AEDC TDR-63-117), Aro, Inc., Aug. 1963.

4. Barton, D. L.; and Overall, B. W.: Results of Simulated Altitude Testing of AGC Subscale Ablatively Cooled Liquid-Propellant Rocket Engines for the Apollo Spacecraft. (AEDC-TDR-63-141), Aro, Inc., Aug. 1963.

5. Anon.: Nozzle Performance Evaluation Program. Final Rep. No. 8289-933002, Bell Aerosystems Co. (NASA CR-56428), 1964.

6. Campell, C. E.; and Farley, J. M.: Performance of Several Conical Convergent-Divergent Rocket-Type Exhaust Nozzles. NASA TN D-467, 1960.

7. Bloomer, Harry E.; Antl, Robert J.; and Renas, Paul E.: Experimental Study of Effects of Geometric Variables on Performance of Conical Rocket-Engine Exhaust Nozzles. NASA TN D-846, 1961.

8. Franciscus, Leo C.; and Lezberg, Erwin A.: Effects of Exhaust Nozzle Recombination on Hypersonic Ramjet Performance: II. Analytical Investigation. AIAA J., vol. 1, no. 9, Sept. 1963, pp. 2077-2083.

9. Sarli, V. J.: Investigation of Nonequilibrium Flow Effects in High Expansion Nozzles. Final Rep. No. B910056-12, United Aircraft Corp. (NASA CR-52921), 1963.

10. Girouard, H.; Graber, F. M.; and Myers, B. F.: Catalysis of Hydrogen Atom Recombination. Final Rep. No. AE63-0078, General Dynamics/Astronautics (NASA CR-52376), 1963.

11. Zeleznik, Frank J.; and Gordon, Sanford: A General IBM 704 or 7090 Computer Program for Computation of Chemical Equilibrium Compositions, Rocket Performance, and Chapman-Jouguet Detonations. NASA TN D-1454, 1962.

"The aeronautical and space activities of the United States shall be conducted so as to contribute . . . to the expansion of human knowledge of phenomena in the atmosphere and space. The Administration shall provide for the widest practicable and appropriate dissemination of information concerning its activities and the results thereof."

—NATIONAL AERONAUTICS AND SPACE ACT OF 1958

NASA SCIENTIFIC AND TECHNICAL PUBLICATIONS

TECHNICAL REPORTS: Scientific and technical information considered important, complete, and a lasting contribution to existing knowledge.

TECHNICAL NOTES: Information less broad in scope but nevertheless of importance as a contribution to existing knowledge.

TECHNICAL MEMORANDUMS: Information receiving limited distribution because of preliminary data, security classification, or other reasons.

CONTRACTOR REPORTS: Technical information generated in connection with a NASA contract or grant and released under NASA auspices.

TECHNICAL TRANSLATIONS: Information published in a foreign language considered to merit NASA distribution in English.

TECHNICAL REPRINTS: Information derived from NASA activities and initially published in the form of journal articles.

SPECIAL PUBLICATIONS: Information derived from or of value to NASA activities but not necessarily reporting the results of individual NASA-programmed scientific efforts. Publications include conference proceedings, monographs, data compilations, handbooks, sourcebooks, and special bibliographies.

Details on the availability of these publications may be obtained from:

SCIENTIFIC AND TECHNICAL INFORMATION DIVISION

NATIONAL AERONAUTICS AND SPACE ADMINISTRATION

Washington, D.C. 20546